Embryology and Early Life History of Rio Grande Silvery Minnow *Hybognathus amarus* (Teleostei: Leuciscidae) with Detailed Morphological Description of Its Larva

Steven P. Platania[1,2], W. Howard Brandenburg[1], and Robert K. Dudley[1,2]

Understanding fundamental life history and ecological attributes of declining endemic fishes is essential for developing effective strategies for their conservation and recovery. In the Great Plains and desert rivers of North America, numerous imperiled leuciscids belong to a unique reproductive ecotype with drifting eggs and larvae (pelagophils). Herein, we synthesize three decades of research on the embryology and early life history of Rio Grande Silvery Minnow *Hybognathus amarus*, a federally endangered member of this ecotype, and explore how our findings can guide management and conservation of these sensitive taxa. We investigated three early developmental aspects of *Hybognathus amarus* through aquarium and laboratory studies: 1) egg morphology, development, and density, 2) larval development, growth, and behavior, and 3) morphologic and meristic analysis of larvae and early juveniles. Eggs nearly doubled in size at 10 min post-fertilization, were nonadhesive and nearly neutrally buoyant (specific gravity: 1.0011–1.0024), and hatched within 30 hrs in water about 23°C. Recently emerged protolarvae first transformed to mesolarvae after about one week, to metalarvae after about three weeks, and to juveniles after about six weeks at 20–24°C. Based on six candidate models, larval fish development (i.e., from protolarvae to early juveniles) was best explained by a cubic polynomial growth curve. While most protolarvae developed a gas bladder and began to feed within a week, the complete complement of fin rays (i.e., required for proficient swimming) had not fully formed until about one month post-hatching. Early developmental characteristics (e.g., egg specific gravity and larval fin ray formation), combined with river fragmentation, flow regulation, and habitat loss, can profoundly affect the upstream retention and recruitment of *Hybognathus amarus* and other native pelagophils. Long-term recovery of these highly imperiled species will depend on restoring sufficient seasonal flows, river and floodplain connectivity, and habitat complexity to promote their successful spawning, growth, and survival.

FEDERALLY endangered Rio Grande Silvery Minnow *Hybognathus amarus* (Girard, 1856) is a pelagic-broadcast spawning leuciscid native to the Rio Grande basin of New Mexico, Texas, and Mexico (USFWS, 1994; Platania and Altenbach, 1998). This species belongs to a reproductive guild of small-bodied, short-lived, freshwater fishes (~15–20 species, family Leuciscidae) that are native to the Great Plains rivers of North America (Platania and Altenbach, 1998; Dudley and Platania, 2007; Worthington et al., 2018). This diverse group of pelagic-broadcast spawning (pelagophils) riverine fishes release nonadhesive, nearly neutrally buoyant eggs into the water column, which are passively transported downstream (Moore, 1944; Balon, 1975; Fausch and Bestgen, 1997; Platania and Altenbach, 1998). During the past century, this assemblage has experienced drastic reductions in distribution and abundance following widespread river fragmentation and flow regulation (Dudley and Platania, 2007; Jelks et al., 2008; Gido et al., 2010; Perkin and Gido, 2011; Perkin et al., 2015). The conservation of native pelagophils is a burgeoning area of ichthyology (Worthington et al., 2018), yet descriptions of their early life histories (e.g., egg morphology, embryology, ontogeny, and growth) are deficient in recent literature (Battle and Sprules, 1960; Bottrell et al., 1964; Sliger, 1967). The biology of nearly neutrally buoyant eggs and drifting larvae (i.e., ichthyoplankton or propagules) is fundamental for assigning species to the correct reproductive guilds, and to understanding the

declines in occurrence and abundance of native pelagophils (Platania and Altenbach, 1998; Fuiman, 2002; Dudley and Platania, 2007; Durham and Wilde, 2008; Worthington et al., 2018).

Hybognathus amarus is one of the most imperiled members of this unique reproductive guild. The remnant wild population of this species currently occurs in approximately 280 river km of the Middle Rio Grande of New Mexico, which only represents ~5% of its historical range (Bestgen and Platania, 1991), and its persistence has partially depended on substantial augmentation with hatchery-reared fish since 2002 (Archdeacon et al., 2023). Including *Hybognathus amarus*, the Middle Rio Grande once sustained five native putative pelagophils that produced nearly neutrally buoyant eggs: Phantom Shiner *Alburnops orca* and Rio Grande Bluntnose Shiner *A. simus simus* are extinct, while Speckled Chub *Macrhybopsis aestivalis* and Rio Grande Shiner *Notropis jemezanus* are extirpated (Bestgen and Platania, 1990, 1991; Platania and Altenbach, 1998). The decline of these taxa as well as federal listing of *Hybognathus amarus* as endangered motivated the first direct observations and classification of spawning behaviors and egg types of several Rio Grande basin leuciscids (Platania and Altenbach, 1998). The discovery of the pelagic-broadcast spawning mode and egg type provided valuable new insights and research directions into the conservation of this reproductive ecotype. Notably, subsequent studies of *Hybognathus amarus* and their pelagic,

---

[1] American Southwest Ichthyological Researchers, L.L.C., 800 Encino Place NE, Albuquerque, New Mexico 87102-2606; ORCID: (SPP) 0000-0001-5290-6603; and (RKD) 0000-0001-9733-563X; Email: (SPP) steven_platania@asirllc.com; (WHB) whburg@gmail.com; and (RKD) robert_dudley@asirllc.com. Send correspondence to SPP.
[2] Division of Fishes, Museum of Southwestern Biology, University of New Mexico, Albuquerque, New Mexico 87131.

nearly neutrally buoyant eggs demonstrated the negative impacts of human-mediated river modifications (i.e., fragmentation and flow regulation) on the survival of drifting ichthyoplankton (Alò and Turner, 2005; Osborne et al., 2005; Dudley and Platania, 2007). Recent studies have since attributed the regional decline of this guild to the interplay of their early life history and water management practices (Gido et al., 2010; Perkin and Gido, 2011; Perkin et al., 2015). However, fundamental descriptions of growth, development, and behavior of early life stages (i.e., egg, embryo, and larva) have not been published for *Hybognathus amarus* or other members of this reproductive guild. Important knowledge of the early life history of this imperiled reproductive ecotype can be gained through the study of representative species, such as *Hybognathus amarus*.

This paper is a synthesis of three separate studies, conducted over three discrete periods, that collectively analyze and describe the morphology, growth, and development of the eggs, embryos, and larvae (along with behavior of the early developmental phases) of *Hybognathus amarus*. The objectives of this synthesis are to: (A) provide comprehensive documentation of egg morphology and embryological development, (B) describe larval development, growth, and behavior, and (C) provide a detailed morphological and meristic diagnosis of larvae and early juveniles. Ultimately, the goal of this paper is to update aspects of the information first presented by Platania and Altenbach (1998). While many post-Platania and Altenbach (1998) publications characterized Great Plains leuciscids based on reproductive mode or spawning strategy (e.g., pelagophilic, lithopelagophilic), we emphasize that the single most important aspect of the reproductive biology of these fishes, and the defining attributes that dictate the long-term persistence of populations, are the joint physical characteristics of the egg, nearly neutral buoyancy, and lack of an adhesive chorion (Platania and Altenbach, 1998; Dudley and Platania, 2007). Our long-standing research on leuciscids in New Mexico continues to focus on egg buoyancy, and subsequent downstream transport (i.e., drift), of the diaphanous eggs of *Hybognathus amarus* (Fig. 1). Our laboratory and field-based research on this reproductive guild, over the past two decades, continues to document the overwhelming importance in understanding the timing of spawning, its relationship to streamflow patterns, and the resultant downstream transport of eggs (i.e., drift). In addition to the detailed accounts presented herein, we discuss this information in context of research on this species and its implications for reproductive success in the Middle Rio Grande. This synthesis of the early life history of *Hybognathus amarus* contributes valuable information and insights related to its conservation and of other riverine leuciscids that produce nonadhesive, nearly neutrally buoyant eggs.

MATERIALS AND METHODS

We studied aspects of embryology and egg density of *Hybognathus amarus* in 2003 (A), while our initial study on larval fish growth, developmental rates, and behavior was conducted in 1994 (B). The morphological and meristic diagnosis of larvae and early juveniles of *Hybognathus amarus* was conducted 2016–2018 (C) using archived cultured material from the 1994 study and supplemented with wild collected individuals. Specimens (including eggs) collected in each

Fig. 1. Photograph of a live egg and embryo of *Hybognathus amarus*, collected in the Middle Rio Grande (NM, Socorro County, Rio Grande at Sevilleta National Wildlife Refuge, La Joya, 7 June 2018; photo by Andrea D. Urioste), illustrating key characteristics (size [ca. 3.7 mm diameter] and clarity [diaphanous]) of nearly neutrally buoyant eggs and embryos emblematic of this reproductive guild.

study were deposited in the Division of Fishes of the Museum of Southwestern Biology (MSB) at the University of New Mexico (UNM) with a subset of original material gifted to the Larval Fish Laboratory at Colorado State University (CSU). Institutional abbreviations follow Sabaj (2020). Common and scientific names follow Page et al. (2023).

A: Embryology and egg density.—Eight female and 14 male *Hybognathus amarus* (collected from the Rio Grande, Socorro County, NM) were injected with carp-pituitary extract (CPE) at 1500 hrs on 8 October 2003, following the procedures outlined in Platania and Altenbach (1998), and maintained in a spawning aquarium (378.5 L) at about 23°C with a salinity of 1.9 ppt. Spawning occurred about 0000 hrs on 9 October 2003. Fertilized eggs were transferred from the spawning aquarium to the UNM confocal microscopy laboratory at 0800 hrs on 9 October 2003 to determine embryological development and physical characteristics. Embryological development was observed on ten eggs, with all embryos at the same initial developmental phase. All specimens were examined, measured, and images obtained using confocal microscopy. The same individual embryo was photographed for almost all developmental images. Preserved samples of post-spawn eggs (15 s, 10 min, 30 min) from the initial study (1994, B) were used to supplement early developmental material. Mean egg diameter and embryo standard length (SL) were measured to the nearest 0.1 mm, per post-spawning period, for all samples. Student's *t*-tests (Student, 1908) were performed per pair to compare post-spawning period mean egg diameters and embryo lengths, blastula/gastrula (10.0–12.5 hrs post-spawn), early embryo/tail-bud (13.7–16.5 hrs), and late embryo (33.0–35.5 hrs) stages.

Live eggs of *Hybognathus amarus* ($n = 100$) for each of the three embryonic stages (blastula/gastrula, early embryo/tail-bud, and late embryo) were used to determine terminal velocity and specific gravity. These eggs were not used in any other phase of investigation because they could not be easily removed from the velocity chamber without causing potential damage and affecting their viability. Terminal velocities of the nearly neutrally buoyant eggs were calculated, after initial acceleration, in a test cylinder filled with distilled water (20°C). The test cylinder was a 183 cm tall × 8.9 cm diameter clear acrylic (6.35 mm thickness) tube sealed at its base and anchored to a plywood board base (1 m^2) for stability. Terminal velocity (mm/s) was determined by the time (0.5 s) required for an egg to descend a vertical distance of 700 mm in the cylinder (from 300–1,000 mm, as measured from the top). Time was initialized at 300 mm (marked on the test cylinder) to ensure eggs had reached their terminal velocity. Specific gravity (SG) of live eggs was calculated following procedures in Dudley and Platania (1999). The SG equation is derived from the difference between the SG of water and the SG of the egg falling through the water (ΔSG) and is represented as:

$$\Delta SG = 0.75(U^2 C_D / Dg)$$

where U is the egg terminal velocity, C_D is the empirical drag coefficient, D is the egg diameter, and g is Earth's gravitational constant ($\sim$9,800 mm/s^2). The empirical drag coefficient (C_D) was estimated using an equation calculated from empirical evidence reviewed in White (2006):

$$C_D = \left(\frac{24}{Re_D}\right) + \left(\frac{6}{1 + Re_D^{0.5}}\right) + 0.4$$

where Re_D is the ratio of inertial forces to viscous forces in a liquid (i.e., Reynolds number). The Reynolds number was calculated as $Re_D = UD/\upsilon$, where υ is kinematic viscosity of water (1.0034 mm^2/s) assuming a density of 998 kg/m^3 and temperature of 20°C (at atmospheric pressure). Mean terminal velocity and specific gravity of live eggs were assessed for the blastula/gastrula (10.0–12.5 hrs post-spawn), early embryo/tail-bud (13.7–16.5 hrs), and late embryo (33.0–35.5 hrs) stages.

B: Egg and larval fish developmental morphology, growth rates, and behaviors.—On 11 May 1994 from 1300 to 1400 hrs, 43 gravid female and 24 ripe male *Hybognathus amarus* were collected at the confluence of the Rio Grande and the North Socorro Diversion Channel (Socorro County, NM; UTM 326501E, 3774731N, Zone 13S). Live specimens were carefully transported to a laboratory at UNM where individuals were examined to determine their relative health, reproductive condition, sex, and age. Fish selected for the study were anesthetized using tricaine mesylate (MS-222) and given an abdominal injection of approximately 0.1 cc (0.11 mg) of acetone-dried CPE to induce spawning. Reproductively capable *Hybognathus amarus* were then placed in an aquarium (378.5 L) where they were observed until they recovered from the anesthesia. Injection of *Hybognathus amarus* collected for this study began at 2300 hrs (11 May 1994) and concluded by 2355 hrs. Specimens remained in the spawning aquarium for about 36 hrs to allow multiple spawning events and to yield many eggs (and subsequent larvae) for developmental studies. The

approximate time between injection, spawning, and hatching was recorded. Aquaria were maintained in a greenhouse in the Department of Biology at UNM that received natural sunlight and maintained a daytime ambient temperature of approximately 27°C. Minimum and maximum water temperatures were recorded daily on submerged minimum-maximum thermometers (Taylor Holdco, LLC). A tubular air-stone (25 cm) was placed in the lower corner of the spawning aquarium to maintain an adequate dissolved oxygen concentration and provide continuous water current. Two aquarium nets (25 × 18 cm, fine mesh) were suspended just below the water surface to collect eggs produced during spawning. Aquarium nets were installed about eight hours after the fish were injected with CPE and checked for eggs every two hours.

Eggs collected in the nets were transferred to a smaller aquarium (189.3 L) for rearing. Compressed air and a tubular air-stone provided air and current in the rearing aquarium. A clear acrylic tray (37 × 15 × 8 cm) suspended 5 cm below the water surface provided a low-velocity rearing habitat (i.e., artificial backwater) for larval fish (Fig. 2). Samples of eggs were preserved in 5% buffered formalin within 15 s of spawning, and at 10 min and 30 min post-spawning intervals. Samples of developing larvae were collected twice daily for the first 12 days following hatching, daily for the following ten days, and then weekly until individuals achieved the juvenile phase. Day 0 was designated as the day that larvae emerged (i.e., hatched). Larval fish were fed finely ground commercial larval fish food twice per day starting on Day 6; diet was supplemented by algae that naturally grew on the interior walls of the aquarium. Observations of larval swimming behavior and the number of larvae present in the artificial backwater were recorded daily during the first week post-hatching.

Preserved (5% buffered formalin) larval specimens were examined in the laboratory for characteristics indicative of selected developmental phases following Snyder (1983). No discernible developmental differences between the two
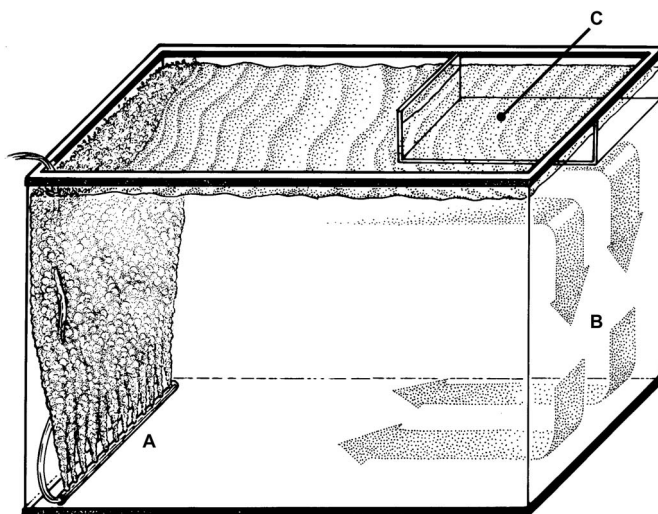
Fig. 2. Illustration of tank used to rear *Hybognathus amarus* from egg to early juvenile stages (189.3 L): (A) shows the 25 cm tubular air-stone used to maintain dissolved oxygen and provide continuous circular flow, (B) indicates flow direction, and (C) is the clear acrylic tray (37 × 15 × 8 cm) that was suspended 5 cm below the water surface to provide low-velocity habitat for larval fish (i.e., artificial backwater).

daily samples taken during days 1–12 was observed; therefore, only one sample per day was selected for study. A stereomicroscope fitted with an ocular micrometer was used to visually examine eggs, embryos, and larval fish; egg diameter and SL were measured to the nearest 0.1 mm. Initial development of crucial morphological features was assessed (e.g., pigmentation, yolk absorption, formation of fin rays). Terminology for reproductive behavior and egg type follow Breder and Rosen (1966) and Balon (1975, 1981).

Six growth models were developed in program R (R Core Team, 2022) to evaluate the relationship between age (in days post-hatching) and SL of larvae and juveniles. Simple linear, quadratic polynomial, and cubic polynomial models were assessed using the base *lm* function in R. More complex sigmoidal logistic, Gompertz (Gompertz, 1825), and von Bertalanffy (von Bertalanffy, 1938) growth models were also assessed using the FSA package (Ogle et al., 2022). Growth models were evaluated using a corrected Akaike information criterion (AIC$_c$; Akaike, 1973), and the model with the lowest AIC$_c$ was considered the most parsimonious. Log likelihood, uncorrected AIC, and Bayesian information criterion (BIC; Schwarz, 1978) values were also calculated per growth model. Daily length measures were compiled as box plots, using SigmaPlot (version 14.5; Systat Software Inc., San Jose, California, 2020), and the first appearances of key morphological features were denoted, as well as the durations that larval developmental phases were present in samples.

C: Morphology and meristic diagnosis of larvae and early juveniles.—Morphological and meristic analysis of larvae and early juveniles of *Hybognathus amarus* ($n = 85$) was performed from 2015 to 2018. Most specimens ($n = 56$) were obtained from materials cultured and archived during the 1994 study (B). In addition, 29 wild larvae of *Hybognathus amarus*, collected from 1996 to 2008 in the Middle Rio Grande of New Mexico, were also incorporated. Four early life-history phases were evaluated: protolarvae ($n = 10$); mesolarvae ($n = 36$), which is comprised of the sub-phases flexion mesolarvae ($n = 17$) and postflexion mesolarvae ($n = 19$); metalarvae ($n = 20$); and early juvenile ($n = 19$). Individual fish were analyzed by developmental phase for up to 24 morphological measures and eight myomere counts, four fin-ray counts, and a suite of pigmentation characters (Figs. 3, 4). Specimens were examined using a stereomicroscope with an ocular micrometer reticle eyepiece and combinations of reflected, transmitted, and polarized light. Calibration of the ocular micrometer was performed with a stage micrometer prior to analyses to ensure accuracy of measures at multiple magnifications. Measurements were made to the nearest 0.1 mm and occasionally to 0.05 mm. Acquisition of morphological data and meristic values, as well as preparation of scientific illustrations, was completed by the same researcher (WHB), thereby maximizing consistency of measures and counts, and accuracy in the representation of the developmental illustrations.

Mean morphological measures were summarized as percent mean SL per developmental phase. Fourteen measures describe body lengths, five measures describe body depths, and five measures describe body widths. Standard length was determined at onset of and at transitions to these important ontogenetic events: larval phase transitions (hatching to early juvenile), gut phase transitions (90° bend to full crossover), onset of eye pigmentation, formation of pectoral- and pelvic-fin buds, loss of yolk and preanal finfold, formation of first and last principal fin rays in each of the median and paired fins, formation of first and last rudimentary rays of the caudal fin, and initial and complete formation of lateral scales on the body.

Pigmentation distribution or pattern was summarized from 49 pigment characters, up to 30 of which were applicable depending on developmental phase. Other diagnostic characters used to describe larvae and early juveniles of *Hybognathus amarus* included eye shape, general mouth position, relative position of posterior corner of mouth, and relative position of fins. Additionally, 20 meristic values were recorded. These characters were comprised of eight myomere counts, lateral line scale counts, number of vertebrae, pharyngeal teeth formula, and counts of principal and rudimentary rays of median and paired fins.

Eight continuous-tone graphite and black-ink illustrations of larvae or early juveniles of *Hybognathus amarus* were prepared in dorsal, lateral, and ventral views to visualize morphological and pigmentation differences among developmental phases. For all illustrations, enlarged composite digital photos of primary, secondary, and tertiary images of specimens were created. Finalized digital image files were printed, and specimen outlines (from digital images) were used to ensure accurate body proportions. Draft illustrations were generated on vellum paper. Graphite and gray ink were used to render most portions of body form, anatomical structures, and shading. Black ink was used for surface or near-surface pigmentation to distinguish it from deeper pigmentation. Body proportions and meristic values in the drawings were verified, and details were added during examination of specimens under a stereomicroscope. If necessary, drawings were idealized (e.g., closed or frayed fins were opened and smoothed, and curved bodies straightened), and melanophore distribution and other structures were modified to represent a prototypical pattern or condition based on secondary and tertiary images of specimens.

RESULTS

Embryology and egg density.—Growth of *Hybognathus amarus* proceeds rapidly through typical teleost embryological stages of development (Fig. 5). Shortly after spawning, the blastomeres of the developing zygote begin rapidly dividing and form a cellular disk (blastoderm) that progressively covers most of the top surface of the yolk. The blastula stage (Fig. 5A) of *Hybognathus amarus* is achieved 6 hrs post-fertilization and is characterized by the linear and hollow mass of blastomeres that form along the top of the yolk. As development proceeds to the gastrula stage (Fig. 5B; 8 hrs post-fertilization), germ layers form and a ring of blastomeres envelopes most of the yolk's circumference. The embryonic axis head and tail are clearly visible by the early embryo stage (Fig. 5C; 10 hrs post-fertilization), while the neural tube, notochord, and somites are in the earliest phases of development and not yet visible. By the tail bud stage (Fig. 5D; 12 hrs post-fertilization), the cephalic region, somites, and caudal region are visible in the developing embryo. During the early part of the tail free stage (Fig. 5E; 14 hrs post-fertilization), the optic vesicle is clearly defined as are the developing somites along the length of the notochord. The tail has grown beyond the yolk mass by the beginning
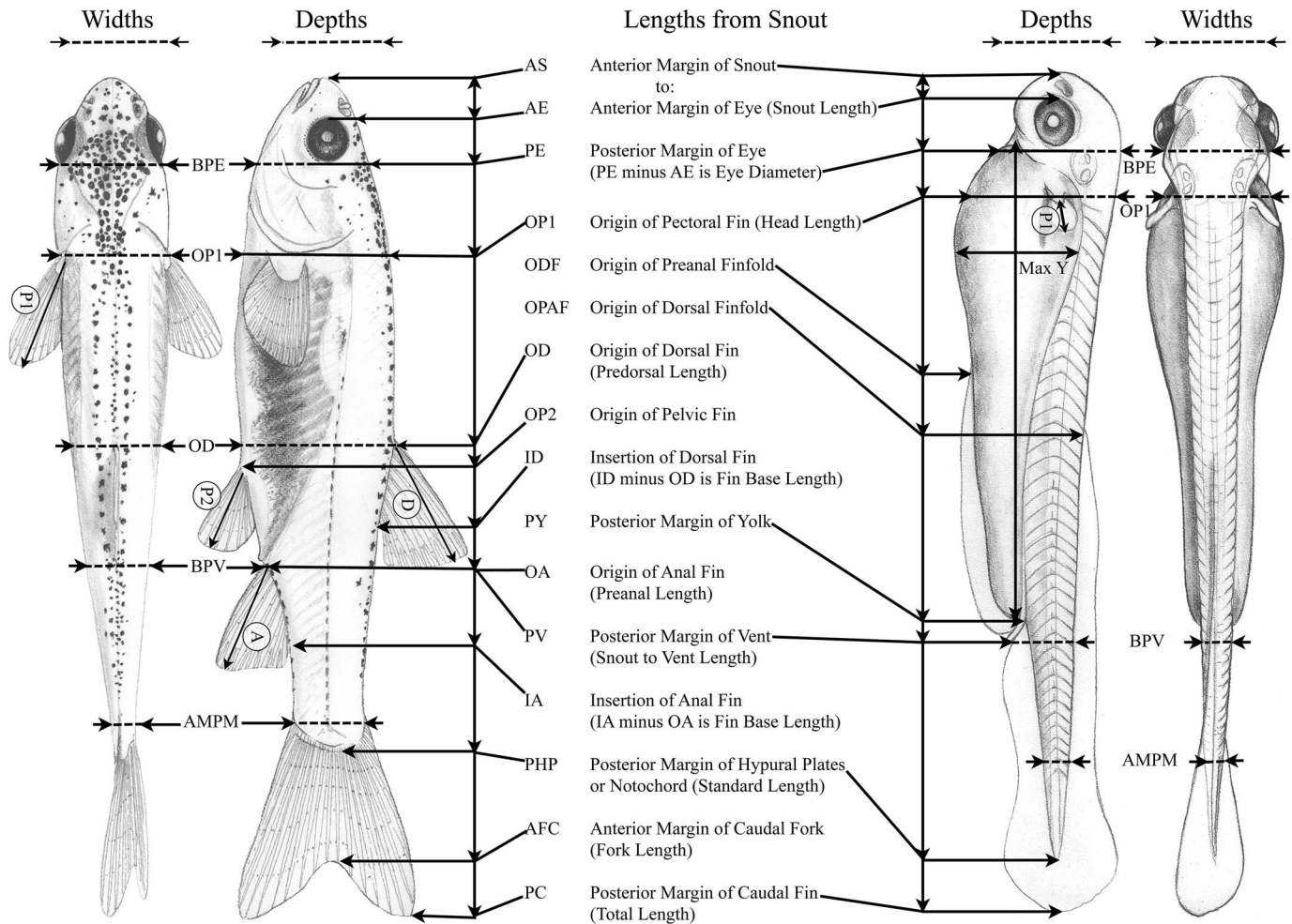
Fig. 3. Measures for larval and early juvenile fishes. Yolk sac (Y) and pterygiophores are included in the width and depth measures but fins and finfolds are not. "B" in BPE and BPV means immediately behind. AMPM is anterior margin of most posterior myomere. PHP is measured to the end of notochord until the adult complement of principal caudal-fin rays is observed (postflexion mesolarval phase). Fin lengths (D, A, P1, and P2, encircled) are measured along the plane of fin from its origin to most distal margin. Images modified from Snyder et al. (2016).

of the late embryo stage (Fig. 5F; 18 hrs post-fertilization), and the auditory vesicle, otoliths (two small black dots within vesicle), myomeres, and Kupffer's vesicle are developed and visible at this stage. At the middle of late embryo stage (Fig. 5G; 22 hrs post-fertilization), the embryo is visible within the confines of the chorion and surrounded by the large protective perivitelline space. The lens of the eye is visible during the middle of late embryo stage and the embryo maintains a large yolk sac. By the end of the late embryo stage (Fig. 5H; 26 hrs post-fertilization), and about 4 hrs prior to hatching, the embryo closely resembles a newly hatched yolk-sac larva (i.e., protolarva).

Egg diameter and embryo length.—From the 1994 reproductive study, we examined 107 fertilized eggs of *Hybognathus amarus* and their embryos (Table 1). Immediately after spawning (0–2 min), mean egg diameter was 1.61 mm ($n = 35$) with mean embryo length of 0.96 mm. At fertilization, the embryo was not uniformly spherical but instead had multiple sharp, angular edges. Another 35 eggs, taken 10 min post-spawning, had significantly expanded in diameter to 2.94 mm ($P < 0.001$), while the embryo achieved a mean length of 1.07 mm ($P < 0.001$). Water diffused into the

perivitelline cavity expanding the chorion, creating a large space between the chorion and embryo, and resulting in a turgid chorion. There were no differences in mean egg diameter ($P > 0.05$) or mean embryo length ($P > 0.05$) between the 10 min and 30 min post-spawn samples. In the 30 min sample ($n = 37$), the embryo was rounded and flattened (saucer-shaped), while the egg was spherical with a smooth chorion and ornamented with a single raised micropyle.

Three samples of eggs ($n = 369$ total) of *Hybognathus amarus* spawned in 2003 were examined for egg and embryo size during later developmental phases. The first sample ($n = 130$) was comprised of eggs that were 10.0–12.5 hrs post-spawning, contained embryos in the blastula/gastrula stages, with mean egg diameter 3.79 mm and embryo length of 1.28 mm. The second sample ($n = 139$) contained eggs at 13.7–16.5 hrs post-spawning and embryos were primarily in the early embryo/tail-bud stage. Embryo length significantly increased to 1.42 mm ($P < 0.001$) compared to the first sample, while the decrease in mean egg diameter (3.73 mm) was not significantly different. In the final 2003 sample ($n = 100$; 33.0–35.5 hrs post-spawning), which was within a few hours of hatching, mean egg diameter was
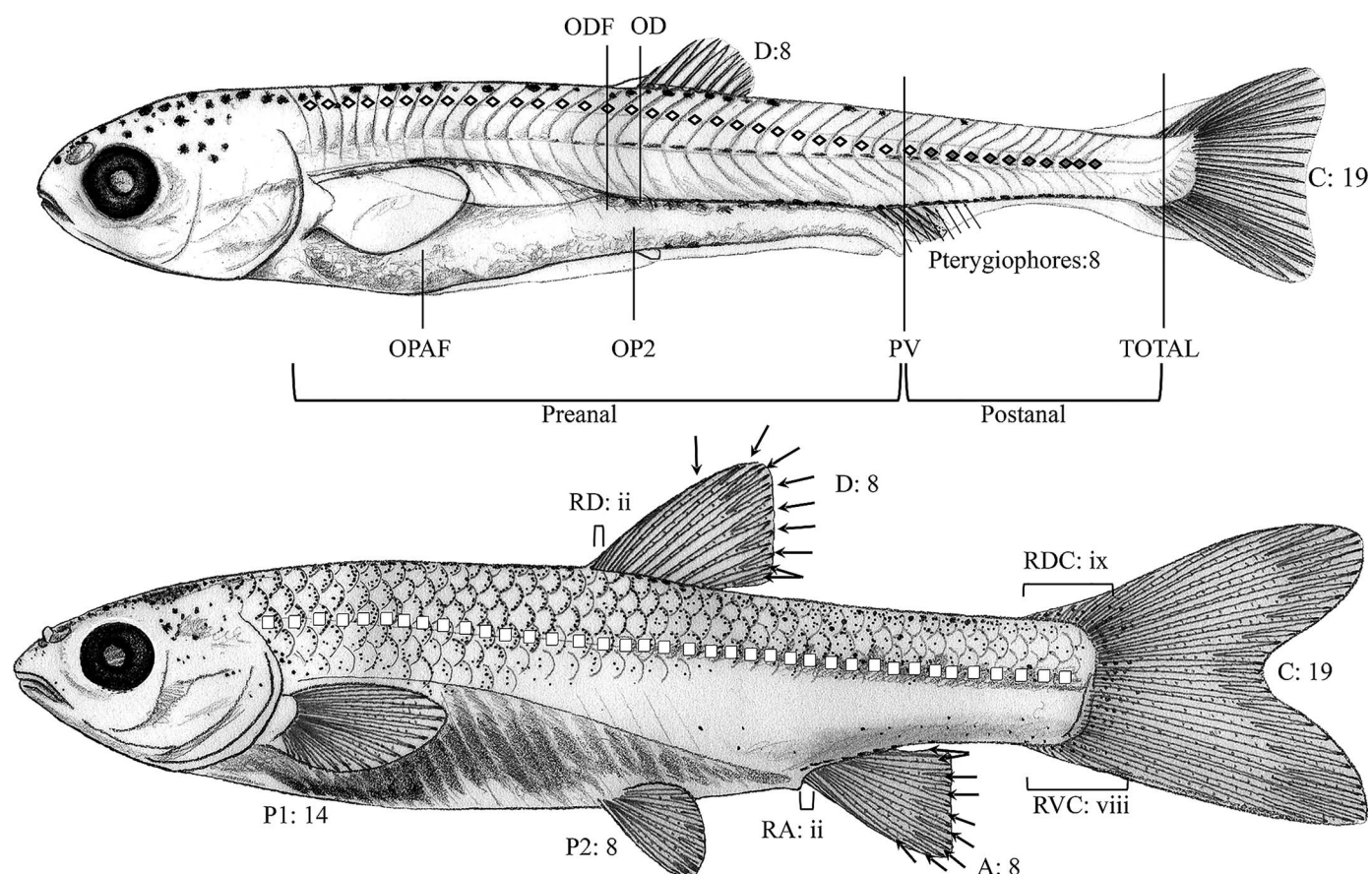
Fig. 4. Meristics (quantitative features) determined for larval and early juvenile cypriniforms. Meristic features comprise myomeres (noted by white diamonds), pterygiophores, fin rays (primary and rudimentary), and lateral line scales (or lateral series if the lateral line is incomplete; noted by white squares). Rudimentary rays are reported in lowercase Roman numerals, while principal median rays are denoted in Arabic numerals; rudimentary rays are not distinguished in paired fins. In the upper illustration, the most anterior and most posterior myomeres included in myomere counts (e.g., ODF, OD, PV) are transected by a vertical line and shaded dark gray. Images modified from Snyder et al. (2016).

slightly smaller (3.62 mm) than the first two samples. Mean embryo length, however, had more than doubled (3.07 mm) and was significantly different than the other two samples ($P < 0.001$).

Specific gravity of eggs.—Terminal velocity and specific gravity of live eggs of *Hybognathus amarus* were estimated from 2003 study material ($n = 300$). Mean egg diameters ($\bar{x} = 3.62–3.79$) and mean embryo lengths ($\bar{x} = 1.21–3.04$) were similar to values obtained for the sample set of 369 eggs (see above section and Table 1). Eggs taken from the 10.0–12.5 hrs post-spawning sample ($n = 100$) descended slowly through the column, taking 105–157 s ($\bar{x} = 128.1$ s; SD = 10.7) to settle 700 mm. Egg terminal velocities were 4.45–6.67 mm/s ($\bar{x} = 5.50$; SD = 0.45). Specific gravity of eggs from the 10.0–12.5 hrs post-spawn sample ranged from 1.0011–1.0024 based on mean egg diameter and terminal velocity. This test was repeated with eggs that were 13.7–16.5 hrs post-spawning ($n = 100$), but egg diameter, terminal velocity, and specific gravity were not significantly different ($P > 0.05$) from the 10.0–12.5 hrs post-spawning sample. The final test was conducted on eggs ($n = 100$) from the 33.0–35.5 hrs post-spawning sample; embryos had progressed to the late embryo stage and were beginning to hatch. Eggs from this sample descended slightly faster than the first two samples, taking 88–134 s ($\bar{x} = 112.3$ s; SD = 8.3)

to travel 700 mm. Compared to values recorded on the first two samples of less developed embryos, egg diameter was smaller ($\bar{x} = 3.62$; $P < 0.001$), embryos were longer ($\bar{x} = 3.04$; $P < 0.001$), terminal velocities were faster ($\bar{x} = 6.27$; $P < 0.001$), and specific gravity was higher ($\bar{x} = 1.0021$; $P < 0.001$) for the third, more developed sample.

Observations.—The newly spawned, nonadhesive eggs of *Hybognathus amarus* dispersed throughout the aquarium and settled to the bottom where they quickly absorbed water and expanded. Perivitelline space (i.e., distance between chorion and embryo; Fig. 6) was minimal upon fertilization but approximately tripled within 10–30 min. As the chorion expanded and the perivitelline cavity filled with water, eggs became nearly neutrally buoyant, rose into the water current, and remained in suspension. Eggs settled to the bottom of the aquaria if water current was not maintained via air stone.

Egg and larval fish development, growth rates, and behaviors.—Laboratory-reared larval and juvenile specimens of *Hybognathus amarus* ($n = 610$) were taken at 31 intervals (in days) after hatching. For each sample, larval phase was determined, and SL was recorded (Fig. 7). Water temperature in rearing tanks ranged from 20–24°C. The number of specimens taken ranged from 8–66 per day ($\bar{x} = 19.7$). The vast
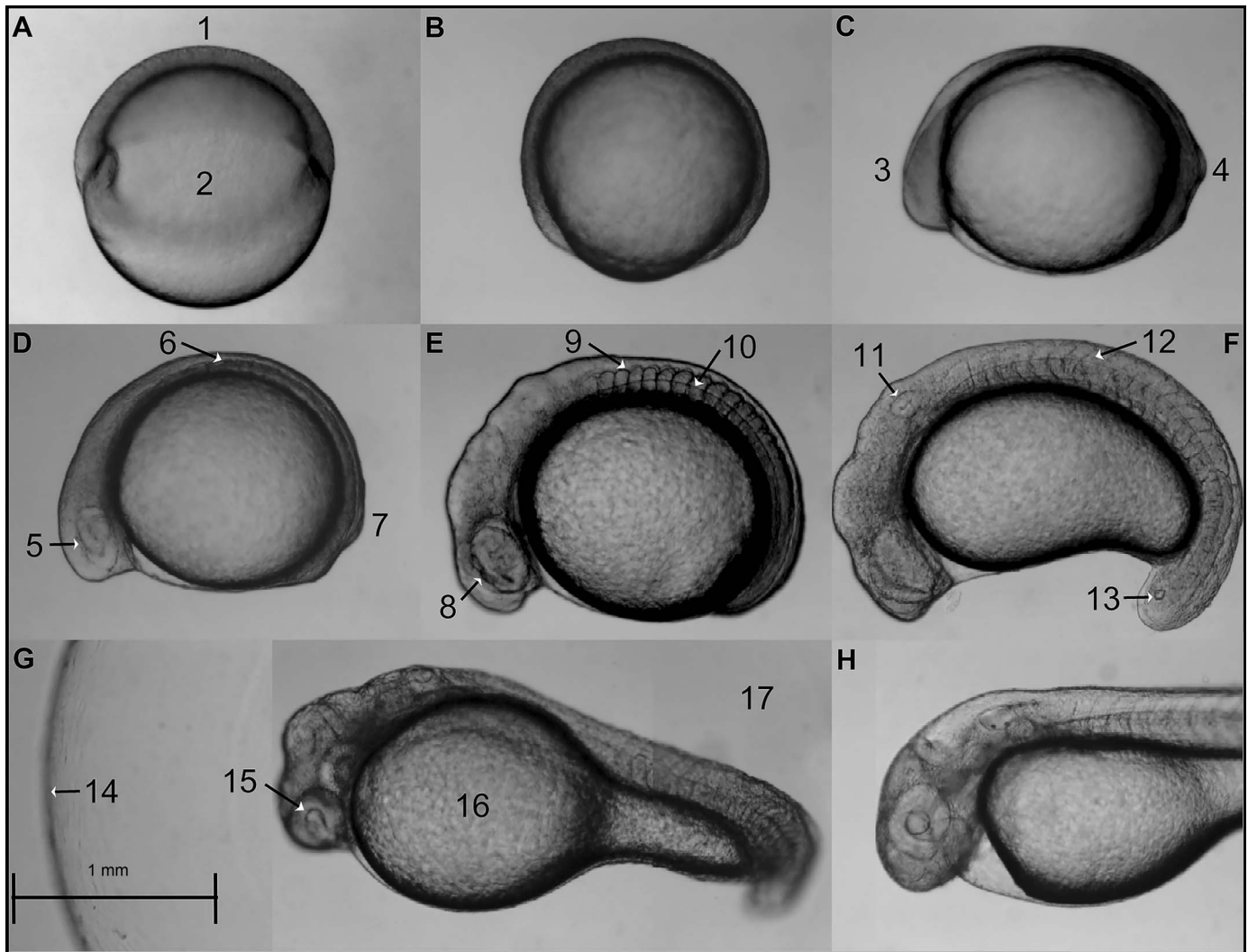
Fig. 5. Developmental phases of *Hybognathus amarus*. Embryonic stage names and anatomical features follow terminology of **Mansueti and Hardy (1967)**. Embryonic stages identified by upper case letters and hours post-fertilization contained in brackets: (A) blastula [6 hrs], (B) gastrula [8 hrs], (C) early embryo stage [10 hrs], (D) tail-bud stage [12 hrs], (E) tail-free stage [14 hrs], (F) beginning of late embryo stage [18 hrs], (G) middle of late embryo stage (composite of two photographs) [22 hrs], and (H) end of late embryo stage [26 hrs], about 4 hrs prior to hatching. Structures that appear throughout embryonic development: 1: blastomeres; 2: yolk; 3: embryonic axis head; 4: embryonic axis tail; 5: cephalic region; 6: somites; 7: caudal region; 8: optic vesicles; 9: developing somites; 10: notochord; 11: auditory vesicle; 12: myomeres; 13: Kupffer's vesicle; 14: chorion; 15: lens of the eye; 16: yolk sac; 17: perivitelline space.

majority ($n = 574$, 94.1%) of individuals examined were either protolarvae or mesolarvae. All protolarvae ($n = 316$) were preflexion, while mesolarvae were either preflexion ($n = 43$), flexion ($n = 36$), or postflexion ($n = 179$). All metalarvae ($n = 29$) and juveniles ($n = 7$) were postflexion. All specimens taken day 0–7 were protolarvae. The first mesolarva was taken on Day 8, but it was not until Day 16 that mesolarvae comprised >50% of the samples. The last protolarva was taken on Day 21, with mesolarval specimens being the most abundant developmental phase until Day 34. The first metalarval specimen was from Day 23. The final sample at a daily interval occurred on Day 27; subsequent samples occurred at one-week intervals. The final daily sample was comprised of 60% mesolarvae and 40% metalarvae; the first weekly sample (i.e., one week later) was comprised of 47% mesolarvae and 53% metalarvae. Metalarval fish were the numerically dominant developmental phase on Day 41, comprising 63% of the specimens with late-mesolarvae

accounting for the remaining 37%. On Day 48, the sample was only comprised of metalarval (46%) and early juvenile (54%) fish.

Recently emerged protolarvae (Day 0) were lacking median fin buds, eye and body pigmentation, and an inflated swim bladder. Specimens had a large yolk sac that extended from the posterior portion of the operculum to the vent. Numerous specimens had slightly curved caudal fins, suggesting that they had only recently hatched. After one day post-hatching (Day 1), yolk sacs appeared smaller but were still the dominant morphological feature and pectoral-fin buds were starting to form. By Day 2, brown eye pigmentation appeared, pectoral-fin buds became fuller, gas bladder formation started, and the yolk sac was being absorbed. The pectoral fins of larval specimens were fully developed by Day 3. Their eyes were well pigmented (i.e., black), body pigmentation was first observed, the gas bladder apparent, and the yolk sac had considerably reduced in

Table 1. Mean, minimum, and maximum egg diameters and embryo lengths of *Hybognathus amarus* at various stages of egg development. Mean, minimum, and maximum egg terminal velocities and specific gravities were also assessed for each stage of development. Egg terminal velocity and specific gravity protocols are discussed in Materials and Methods. Calculations of specific gravity follow Dudley and Platania (1999). Development stages were: blastula/gastrula (BG: 10.0–12.5 h), early embryo/tail-bud (EE: 13.7–16.5 h), and late embryo (LE: 33.0–35.5 h). Samples from 1994 were included to supplement early post-spawn development (0–30 min) and recently hatched protolarvae (PR).

Date	Time post-spawn	Eggs (n)	Egg diameter (mm) Mean (± SD)	Egg diameter (mm) Min–Max	Embryo length (mm) Mean (± SD)	Embryo length (mm) Min–Max	Egg terminal velocity (mm/s) Mean (± SD)	Egg terminal velocity (mm/s) Min–Max	Specific gravity Mean (± SD)	Specific gravity Min–Max
12 May 1994	0–2 min	35	1.61 (0.11)	1.4–1.9	0.96 (0.07)	0.8–1.1	—	—	—	—
12 May 1994	10 min	35	2.94 (0.50)	1.5–3.6	1.07 (0.09)	0.9–1.4	—	—	—	—
12 May 1994	30 min	37	2.90 (0.40)	2.0–3.6	1.12 (0.13)	0.9–1.4	—	—	—	—
9 Oct 2003	10.0–12.5 h	130	3.79 (0.23)	3.2–4.3	1.28 (0.13)	0.9–1.5	—	—	—	—
9 Oct 2003	13.7–16.5 h	139	3.73 (0.26)	3.1–4.2	1.42 (0.20)	1.0–1.8	—	—	—	—
10 Oct 2003	33.0–35.5 h	100	3.62 (0.23)	3.0–4.1	3.07 (0.28)	2.1–3.7	—	—	—	—
9 Oct 2003	10.0–12.5 h	100 BG	3.79 (0.27)	3.2–4.4	1.21 (0.16)	0.9–1.5	5.50 (0.45)	4.45–6.67	1.0016 (0.0003)	1.0011–1.0024
9 Oct 2003	13.7–16.5 h	100 EE	3.79 (0.24)	3.1–4.3	1.43 (0.19)	1.0–1.7	5.52 (0.43)	4.43–6.54	1.0016 (0.0002)	1.0012–1.0022
10 Oct 2003	33.0–35.5 h	100 LE	3.62 (0.22)	3.0–4.2	3.04 (0.27)	2.3–3.5	6.27 (0.49)	5.22–7.95	1.0021 (0.0003)	1.0016–1.0034
14 May 1994[1]	49.5 h	66 PR	—	—	3.71 (0.14)	3.3–3.9	—	—	—	—

[1] All eggs had hatched; data are for 66 recently hatched protolarvae (PR, not embryos).
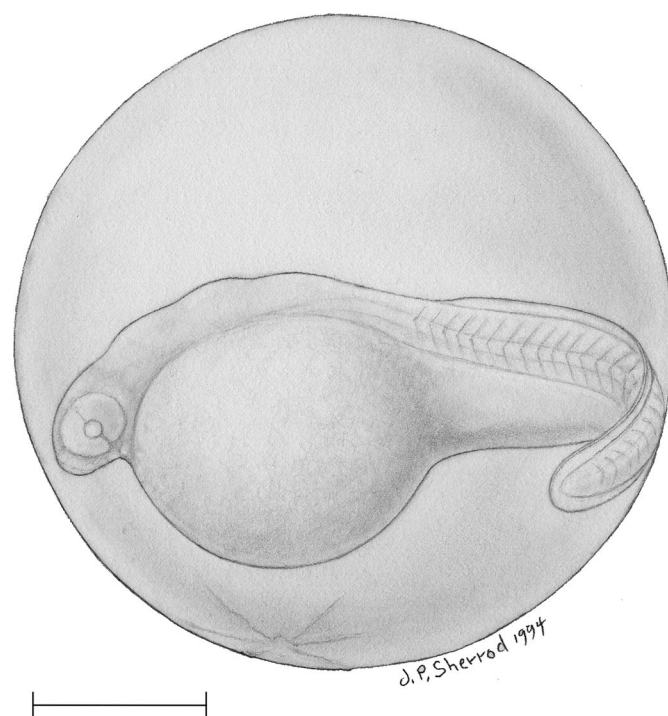

Fig. 6. Illustration of nearly neutrally buoyant egg of *Hybognathus amarus* with large, heavily yolked, almost fully developed embryo, large perivitelline space, and star-shaped micropyle. Bar is 1 mm.

volume. Food was first observed in the gut of larvae on Day 4, which coincided with absorption of the yolk sac. Pigmentation was scattered over the body, with some pigmentation present on the tail, and the pectoral fins were full and contained rays. For the next several days (Days 4–8), there were few major developmental changes as fish proceeded through the protolarval phase to the mesolarval phase. Larvae grew relatively slowly as they absorbed their remaining yolk, started to feed, became deeper bodied, and grew caudal-fin rays. Differentiation of the rays in the dorsal fin was first noted on Day 13, while anal-fin ray differentiation was not observed until Day 17. As fish progressed through the mesolarval phase, the flexion of the notochord completed, fish acquired additional body pigmentation, and medial fin rays formed and segmented. The appearance of pelvic-fin buds on a Day 23 specimen also marked the first metalarval specimen. On Day 24, all larval specimens were strongly pigmented. Most specimens had some dorsal-fin rays but lacked anal-fin rays. However, the largest fish in this sample had a short gut coil near the vent and almost all its principal anal-fin rays. Coiling of the gut was apparent by Day 41 and associated only with metalarval specimens. Fish were feeding on commercial fish food and grazing on algae growing in the aquarium. Growth rate of metalarvae and development of the full complement of pelvic-fin rays was slow. On Day 48, over half of the sample was juvenile fish. These specimens had the full complement of fin rays, fully developed pelvic fins, beginning of a scale pattern, well-segmented medial fin rays, and no remnants of finfolds.

Larval fish early swimming behavior.—Swimming behavior of recently hatched (Day 0) larvae was characterized by vertical movement through the water column (i.e., swim-up behavior). Larvae spent 1–3 s swimming toward the surface, then stopped, began to settle toward the bottom, then reinitiated
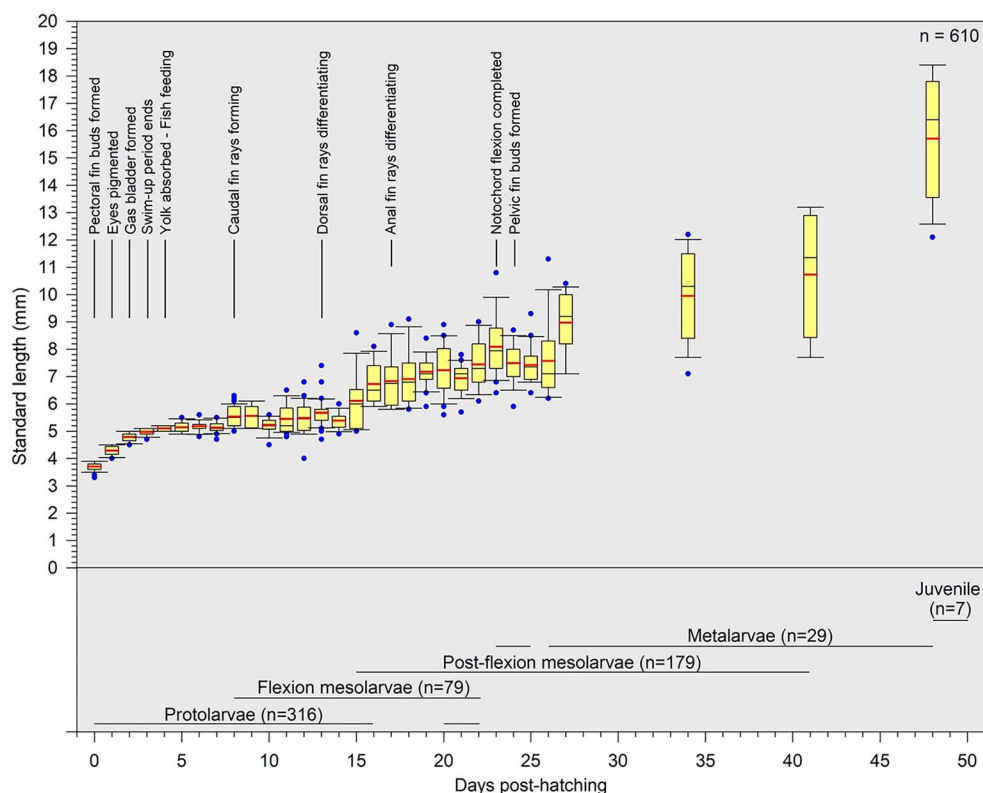
Fig. 7. Box plots representing daily lengths of larvae and early juveniles of *Hybognathus amarus* over 48 days. The box and its associated components represent all lengths, regardless of developmental phase, recorded during a single day. Boxes show the interquartile range (*IQR*; Q_3–Q_1), with the lower and upper bounds of the box respectively representing the first (Q_1; 25th percentile) and third (Q_3; 75th percentile) quartiles. Whisker caps represent the 10th (Q_0) and 90th (Q_4) percentile values, while the thin, black horizontal line (often obscured) represents the median (Q_2; 50th percentile). Red horizontal lines represent the mean lengths; outliers are shown as individual blue dots. The day notable morphological features first appeared are indicated, as well as the range of days each larval phase occurred in the sample.

the sequence after a few seconds. Larvae that contacted the aquarium bottom immediately resumed the sequence of vertical swimming. On Day 1, there were 83 larvae in the artificial backwater (30 mm deep; Fig. 2), and the behavior of specimens in this habitat was different compared to the larvae in the main aquarium. Larvae in the backwater did not attempt to maintain their position in the middle of the water column but instead lay on their sides infrequently swimming toward the surface. On Day 3, of the 143 larvae in the backwater 50% were resting upright, 25% were laying on their side, and the remainder of the fish were tilted between those positions. Fish in the main aquarium stayed in suspension in the current and continued their behavior of vertical movement in the water column. By Day 4, there were 122 fish in the artificial backwater with most of the specimens resting in an upright position. Many larvae in the main portion of the aquarium had abandoned their vertical swimming behavior and were instead swimming horizontally. This horizontal movement coincided with the development of the gas bladder and allowed larvae to move between areas with high and low water velocities. For the next several days, specimens were distributed throughout the aquarium moving freely between the main tank and backwater.

Larval fish growth rate.—Six candidate growth models were assessed to describe the relationship between larval fish lengths (SL) and age (days post-hatching). Models were evaluated by comparing AIC_c values (Table 2). A cubic polynomial growth curve had the lowest AIC_c score (1524.40) and was considered the best fit model given the data. This model also had the lowest BIC and highest log likelihood scores. The predictive growth curve that best fit the raw data (Fig. 8) was described by the cubic polynomial equation ($R^2 = 0.854$):

$$SL = 3.93 + 0.205\text{Age} - 4.89(10^{-3})\text{Age}^2 + 1.16(10^{-4})\text{Age}^3$$

The von Bertalanffy growth equation was the worst fit model ($AIC_c = 1712.19$, $\Delta AIC_c = 187.79$).

Larvae had the smallest variance in body length (SL) within the first week post-hatching (Days 0–7), while specimens taken the last three days (Days 34, 41, and 48) had the greatest variance (Fig. 8). Larval fish exhibited minimal growth between Days 7–14, as they transformed from protolarvae to mesolarvae, but showed greater variability in lengths compared to the previous week. Mean lengths greatly increased as larvae progressed through the mesolarval phase (Days 15–23; 6.11–8.10 mm SL) but increased only slightly during their transition from mesolarvae to metalarvae (Days 23–26; 7.75–8.10 mm SL). Mean SL again increased markedly as larvae progressed through the metalarval phase into the early juvenile phase (Days 27–48; 15.71–89.81 mm SL).

## Morphology and meristic diagnosis of larvae and early juveniles

Morphology.—Egg diameter of *Hybognathus amarus* ranged from 3.62 to 3.79 mm at 10 hrs post-spawning to hatching. Upon hatching, larvae of *Hybognathus amarus* are approximately 4 mm TL (Table 3). Pectoral-fin buds are scarcely visible before hatching but lengthen rapidly just prior to and after hatching (Table 4). The caudal fin is the first to initiate formation of rays (5–6 mm SL), with rays developing sequentially from the lower hypural plate dorsally. Median fin rays develop during the postflexion mesolarval subphase, after the full complement of caudal-fin rays are formed. Dorsal-fin rays are the next to initiate formation (7 mm SL), followed by anal-fin rays (8 mm SL), and finally pectoral- and pelvic-fin rays (9–10 mm SL). In metalarval

Table 2. Comparison of six growth models to evaluate the relationship between age and standard length (SL) of larvae and early juveniles of *Hybognathus amarus*. Three simple models were assessed (cubic polynomial, quadratic polynomial, linear), as well as three more complex sigmoidal models (logistic, Gompertz, VBGE). Growth models were evaluated, considering the number of parameters (K), using a corrected Akaike information criterion (AIC$_c$; Akaike, 1973) and the model with the lowest AIC$_c$ value was considered the most parsimonious. AIC$_c$ differences (ΔAIC$_c$) and weights (AIC$_c$ Wt), and log-likelihood (LogLik) values were estimated per model. Other criteria were assessed and corroborated the AIC$_c$ estimates; uncorrected Akaike information criterion (AIC) and Bayesian information criterion (BIC; Schwarz, 1978).

Model name	K	AIC$_c$	ΔAIC$_c$	AIC$_c$ Wt	LogLik	AIC	BIC	Model equation
Cubic polynomial	5	1524.40	0.00	1.000	−757.15	1524.30	1546.37	$SL = 3.93 + 0.205Age - 4.89(10^{-3})Age^2 + 1.16(10^{-4})Age^3$
Logistic[1]	4	1553.21	28.81	0.000	−772.57	1553.14	1570.80	$SL = 8.02 * 10^3/1 + e^{-2.65 \times 10^{-2} * (Age-2.86 * 10^{-2})}$
Gompertz[1]	4	1556.15	31.75	0.000	−774.04	1556.09	1573.74	$SL = 9.32 * 10^9 * e^{-e^{-1.27 \times 10^{-3} * (Age-2.42 * 10^{-3})}}$
Quadratic polynomial	4	1570.09	45.69	0.000	−781.01	1570.02	1587.68	$SL = 4.25 + 8.54 * 10^2Age + 2.73 * 10^{-3}Age^2$
Linear[2]	3	1710.13	185.72	0.000	−852.04	1710.09	1723.33	$SL = 3.66 + 0.187Age$
VBGE[2]	4	1712.19	187.79	0.000	−852.06	1712.12	1729.77	$SL = 4.58 * 10^4 * (1-e^{-4.08 * 10^{-6} * (Age + 19.65)})$

[1] Gompertz (1825)
[2] von Bertalanffy growth equation (von Bertalanffy, 1938)
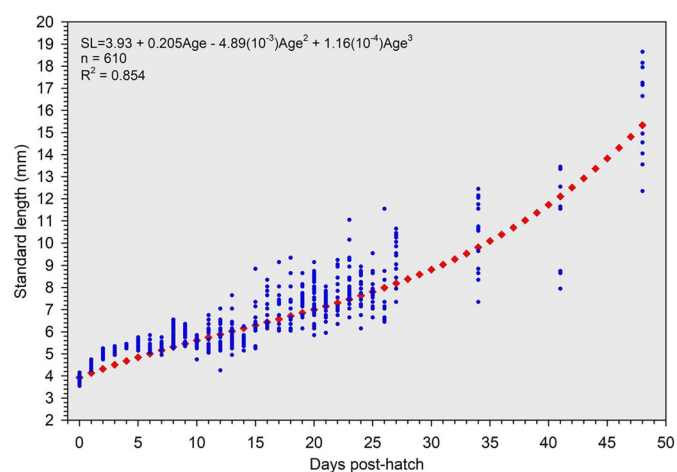
Fig. 8. Body length growth of *Hybognathus amarus* across 48 days. The relationship between SL and age, in days, was best fit by a cubic polynomial model (see Table 2). Raw data points (SL per day, blue circles) are plotted, with model-predicted values (red diamonds).

and early juvenile specimens, the origin of the dorsal fin is clearly anterior relative to the origin of the pelvic fin. Likewise, the posteriormost ray of the dorsal fin (dorsal-fin insertion) is distinctly anterior to the posterior margin of the vent. One species-specific characteristic noted during examination of larval *Hybognathus amarus* that greatly aided in identification of this species was vent location as a proportion of SL (>70% SL). Scale formation is not until the early juvenile phase (ca. 15 mm SL) but is rapid and fully complete by 16–18 mm SL.

Eye shape of *Hybognathus amarus*, a slight oval from embryo to flexion mesolarva, becomes round or nearly round for the remainder of larval and juvenile phases. The eye is lightly colored upon hatching but within one to two days becomes well pigmented and black. Upon hatching, the yolk is primarily a large mass extending ventrally from mid-eye, posterior to the vent. From there, the yolk continues as a finger-like projection that narrows posteriorly. Yolk of embryos and recently hatched larvae are generally opaque with no indication of an oil globule or venation. The developing head of larvae is deflected over the anterior portion of the yolk but separates as the yolk is rapidly absorbed within days of hatching (ca. 5 mm SL).

Mouth position of flexion mesolarval to metalarval phases of *Hybognathus amarus* is terminal and moderately oblique. Lips are usually even with the most anterior margin of snout or sometimes slightly behind the anterior margin of snout. Upon achieving the early juvenile developmental phase, the mouth position is subterminal and slightly oblique to horizontal, with the lips preceding or overhanging the anterior margin of snout. By 5 mm SL, *Hybognathus amarus* have formed a swim bladder and, along with its developing pectoral fins, are within a few days of being able to maintain movement through three axes.

Protolarvae transform to flexion mesolarvae at 5–6 mm SL, while notochord flexion occurs at approximately 6 mm SL, and the metalarva phase is achieved at about 9 mm SL (Table 5). The early juvenile life phase is reached at 13–14 mm SL. *Hybognathus amarus* is an omnivore consuming algae, plankton, diatoms, and organic sediment and has a long, extremely

Table 3. Summary of morphology and myomere counts by developmental phase for *Hybognathus amarus* (n = 85). See **Figures 3** and **4** for abbreviations and methods of measurement and counting. Protolarvae with unpigmented eyes were excluded. Standard deviation [SD] of 0 is a value < 0.5, blank = not applicable. When different than *n*, the number of specimens examined is footnoted.

	Protolarvae (n = 10)			Flexion Mesolarvae (n = 17)			Postflexion Mesolarvae (n = 19)			Metalarvae (n = 20)			Early Juvenile (n = 19)		
	$\bar{x}$	±SD	Range	$\bar{x}$	±SD	Range	$\bar{x}$	±SD	Range	$\bar{x}$	±SD	Range	$\bar{x}$	±SD	Range
Lengths %SL															
AS to AE	3	0	2–3	3	0	3–4	4	0	3–5	5	1	4–6	5	1	4–6
PE	10	1	9–11	11	1	10–12	11	1	10–12	12	1	11–13	12	1	10–13
OP1	18	1	17–20	21	1	20–23	22	1	20–23	25	1	22–28	26	1	23–28
OP2							51	1[c]	51–52	55	2	53–58	56	2	54–59
PY	64	6[a]	56–69												
OPAF	33	6	27–50	32	2	30–37	32	3	25–37	43	10	30–61			
ODF	42	2	38–45	45	2	42–49	48	3[d]	42–52	50	2[b]	48–54			
OD							53	1[e]	51–54	54	1	52–56	53	1	52–56
ID							62	1[e]	60–63	63	1	61–65	65	1	63–66
PV	71	1	69–72	72	1	70–75	74	1	72–75	74	1	71–76	72	1	70–74
OA							73	1[a]	71–74	73	1	70–75	73	1	71–74
IA							79	1[a]	78–81	81	1	78–83	81	2	79–83
AFC							110	1	109–112	113	2	110–116	116	2	112–120
PC	106	1	105–107	107	2	105–111	113	3	109–119	120	2	116–124	127	3	122–131
Depths %SL															
at BPE	14	1	13–15	14	1	13–15	15	1	13–17	17	1	15–18	16	2	14–19
OP1	14	1	13–15	15	1	13–16	16	1	15–19	19	2	14–23	21	1	18–23
OD	11	1	10–12	11	1	10–13	13	1	12–17	19	3	14–23	22	2	18–25
BPV	7	1	6–8	7	1	6–8	9	1	7–11	12	1	10–14	16	1	13–18
AMPM	3	1	2–4	4	1	3–5	6	1	4–7	7	1	6–9	10	1	8–12
Widths %SL															
at BPE	13	1	12–14	13	1	12–14	15	1	13–17	16	1	13–17	15	2	13–18
OP1	10	1	9–13	10	1	8–12	13	1	11–16	15	2	11–18	17	1	15–19
OD	6	1	4–8	7	1	5–8	9	1	6–11	12	2	8–16	15	2	12–18
BPV	5	1	4–6	5	0	4–6	6	1	4–8	8	1	7–10	10	1	8–13
AMPM	2	1	1–3	3	1	2–4	4	1	3–5	4	1	3–6	4	1	3–5
Myomeres															
to PY	24	3[a]	20–27												
OPAF	10	3	6–16	8	1	6–11	6	1	5–8	11	5	6–20			
OP2							17	0[c]	16–17	17	1	16–19	17	1[i]	16–18
ODF	14	1	12–16	14	1	12–16	15	1[d]	13–16	15	1[i]	13–16			
OD							17	1[g]	16–18	16	1	15–18	16	1[i]	15–16
PV	27	1	26–28	27	1	26–29	27	1	26–29	26	1	25–27	26	1[i]	25–27
Total	38	1	36–39	38	1	37–39	37	1	35–39	36	1	35–37	36	1[i]	35–37
After PV	11	1	10–12	11	1	10–12	10	1	9–11	10	1	9–11	10	1[j]	9–11
Fin rays															
P1	11	2	6–12	12	1	10–13	13	1	11–14	14	1	12–17	18	2	14–22
P2							1	1	0–3	7	3[h]	2–11	14	2	11–17
D							12	1[f]	11–13	16	2	13–19	22	2	19–24
A							8	1[a]	7–9	11	1	8–14	16	1	14–17

[a] n = 4, [b] n = 9, [c] n = 5, [d] n = 17, [e] n = 12, [f] n = 11, [g] n = 13, [h] n = 16, [i] n = 8, [j] n = 10

coiled gut like other members of this trophic guild. The gut achieves a 90° bend as early as 7 mm SL and is present at 8–9 mm SL, while a full gut loop appears at 9 mm SL (Table 5). A partial gut crossover first occurs at 9–10 mm SL, while the full crossover of the gut is present by 12 mm SL.

Meristics.—The mean number of myomeres for early life phases of *Hybognathus amarus* (protolarvae and flexion mesolarvae) was 38 (range 36–39), while for later phases (metalarvae and early juvenile) mean myomere count was 36 (range 35–37). There was a similar pattern (reduction in the number in later developmental phases) with preanal myomeres, as the three earliest life phases contained a mean of 27 myomeres (range 26–29), while metalarvae and early juvenile mean preanal myomere count was 26 (range 25–27). Postanal myomeres ranged from 9 to 11 with a mean of 11 in the first two life phases and 10 in later phases. There were 12–16 myomeres anterior to the origin of the dorsal finfold ($\bar{x}$ = 14) and 15–18 myomeres

Table 4. Size at onset of selected developmental events for *Hybognathus amarus*. P = principal rays; R = rudimentary rays. Scales are lateral series. Rare values in parentheses. * Before hatching.

Event–structure	Formation (mm SL)	Fin rays or scales	First formed (mm SL)	Last formed (mm SL)
Hatched	(3) 4 (5)	Dorsal–P	(6) 7 (8)	(7) 8
Eyes pigmented	(4) 5	Anal–P	(7) 8	9 (10)
Yolk assimilated	5	Caudal–P	5–6	(6) 7 (8)
Finfold absorbed	13–14	Caudal–R	7–8	(11) 13
Pectoral-fin buds	(*) 4	Pectoral	9 (10)	(11) 12 (13)
Pelvic-fin buds	9 (10)	Pelvic	9–10	11–13
		Scales	(14) 15	15–18

anterior to the origin of the dorsal fin ($\overline{x} = 16$). The mean number of myomeres from the snout to the origin of the pelvic fin was 17 for all life phases, once the pelvic fin was present (Table 6).

The number of vertebrae in *Hybognathus amarus* ranged from 36 to 37 while the mean number of lateral series scales was 36, but ranged from 34 to 37, rarely 38. Median fin-ray counts, from anterior to posterior, were eight primary dorsal and two rudimentary rays, 7–8 ($\overline{x} = 8$) primary and two rudimentary anal-fin rays, and 19 primary caudal-fin rays (8–10 rudimentary dorsal caudal rays, 8–9 rudimentary ventral caudal rays). Pharyngeal tooth count was 0,4–4,0 (Table 6).

Pigmentation.—Hybognathus amarus is relatively lightly pigmented, especially prior to achieving the early juvenile phase. There is light pigmentation over the midbrain and hindbrain region anterior and posterior to the middle of the eyes. Melanophores are absent (or very sparse) on the ventral surface from the gular region to the vent with no distinct lines or rows of melanophores.

Pigmentation on the dorsal surface of the body, between the head and last myomere, are scattered over all or most of the back with at least a partial, lengthwise row of melanophores on either side of the dorsal midline becoming more defined in later larval life phases. A scattered to distinct midline row of melanophores is also present anterior to the origin of the dorsal fin, extending the full length to the origin of the dorsal in early juveniles. In all larval phases, pigmentation of the horizontal myosepta is moderate to strong along the middle and posterior body forming a light line in later larval phases. Pigmentation outlining scales was scarce to moderate and only present in later stage early juvenile specimens. Subsurface pigmentation of the peritoneum is dense in metalarvae and early juveniles.

Unlike many other leuciscids, there was not a distinct spot or dense aggregation of pigment at the origin or lateral to the dorsal fin. Pigmentation in the dorsal fin was absent during early development but present along principal fin rays in later phases. In metalarval and early juvenile phases of *Hybognathus amarus*, pigmentation is present under or immediately along the base of the dorsal and anal fin. Pigmentation in the pectoral and pelvic fins was generally absent or at most, very light. Pigmentation was absent from the anal fin but present to extensive along principal caudal-fin rays. A faint basicaudal spot, evident in some individuals, is more often absent. Illustrations of larvae and early juveniles of *Hybognathus amarus* provide visual representation of changing morphology through early developmental phases (Figs. 9, 10).

DISCUSSION

Our research comprised three discrete, interrelated studies that in combination provide the most comprehensive documentation to date on the early life history of *Hybognathus amarus*. This work is the culmination of over 20 years of research focused on conservation of this federally endangered fish and its unique reproductive strategy. Knowledge gained through examination of *Hybognathus amarus*, an intensely studied, extant member of a reproductive guild of leuciscid pelagophils, is valuable for understanding needs of numerous species, many of which have experienced declines in their distribution and abundance. Here we discuss our study of early life phases of *Hybognathus amarus* in context of the body of research on other leuciscid pelagophils and explore implications for conservation of the remaining wild population based on extensive knowledge gained from

Table 5. Size at developmental interval and gut phase transitions for *Hybognathus amarus*.

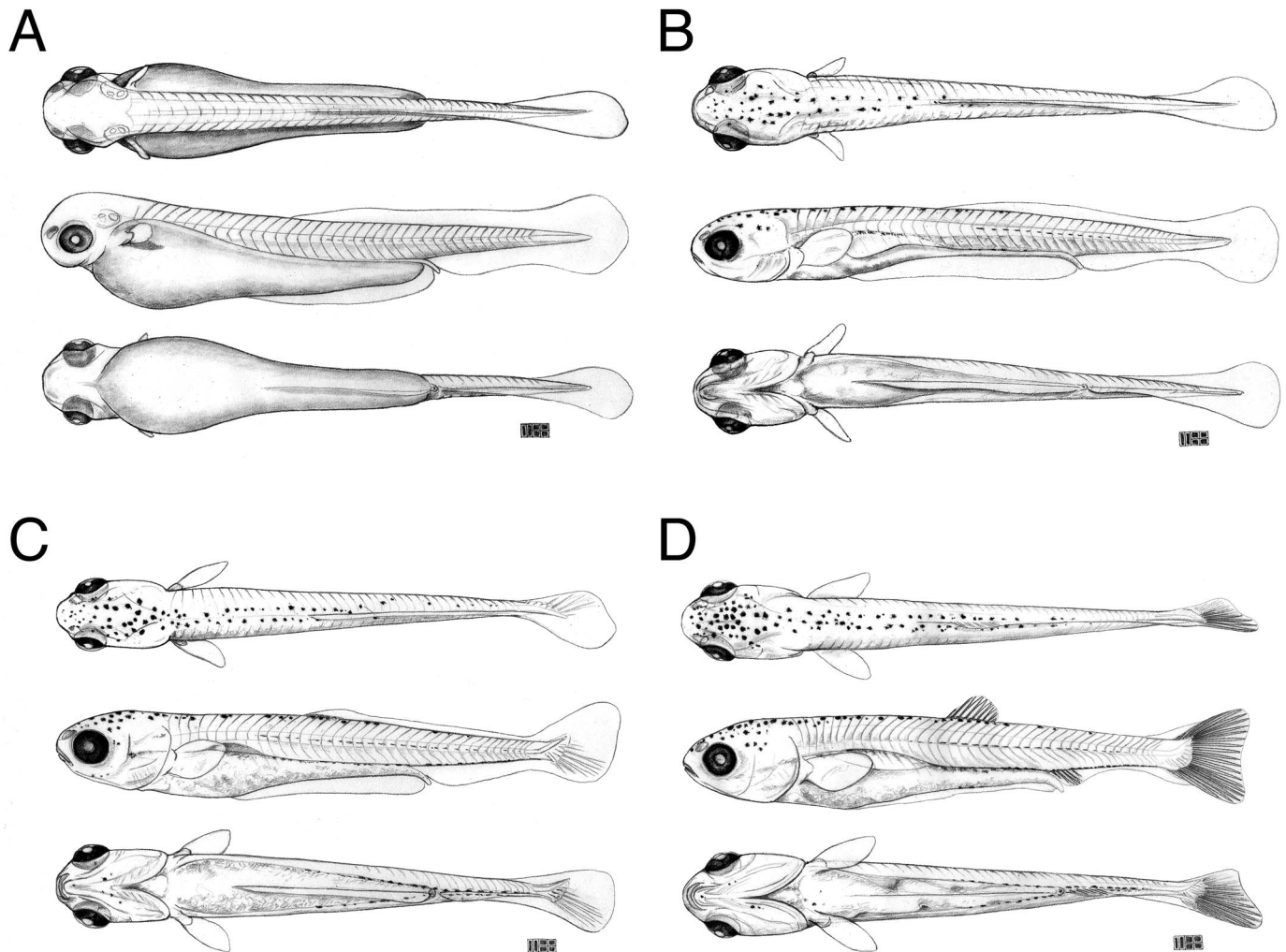| Transition to	mm SL
Flexion mesolarva	5–6
Postflexion mesolarva	(6) 7 (8)
Metalarva	9 (10)
Early juvenile	13–14
2—90° bend	(7) 8–9
3—Full loop	9
4—Partial crossover	9–10 (11)
5—Full crossover	(11) 12

Table 6. Selected early juvenile and adult meristic values for *Hybognathus amarus*. P = principal rays; R = rudimentary rays; D = dorsal; V = ventral). Mean or modal values underlined, rare values are in parentheses. Four added to vertebral count for Weberian complex. Scales are lateral series or lateral line when complete. Pharyngeal teeth given as left outer row, left inner row–right inner row, right outer row.

Character	Number
Dorsal-fin rays–P	(7) 8
Dorsal-fin rays–R	2
Anal-fin rays–P	7–8
Anal-fin rays–R	2
Caudal-fin rays–P	(18) 19
Caudal-fin rays–RD	(8) 9–10
Caudal-fin rays–RV	8 (9)
Pectoral-fin rays	13–14 (15)
Pelvic-fin rays	7–8
Vertebrae	36–37
Lateral scales	34–36–37 (38)
Pharyngeal teeth	0,4–4,0

Fig. 9. Dorsal, lateral, and ventral views of *Hybognathus amarus* (MSB 49967): (A) recently hatched protolarva, 4.7 mm SL, 5.0 mm TL; (B) protolarva, 5.4 mm SL, 5.7 mm TL; (C) flexion mesolarva, 6.0 mm SL, 6.5 mm TL; (D) postflexion mesolarva, 7.2 mm SL, 7.9 mm TL. Rectangular icon below images is the artist's stylized initials.

nearly three decades of field-based monitoring and research we conducted on this imperiled species.

Reproductive terminology of species formerly referred to as "pelagic-broadcast spawners"

We use this inclusive study on the early life history of *Hybognathus amarus* to revisit and refine terminology previously applied by Platania and Altenbach (1998) regarding spawning mode and egg properties. We no longer use the term "pelagic-broadcast spawner" to refer to guild members but instead use pelagophil, which has become common in recent literature (e.g., Horwitz et al., 2018; Worthington et al., 2018; Mollenhauer et al., 2021; Taylor and Mayes, 2022). Likewise, we have modified the terminology previously used to describe egg buoyancy (i.e., semibuoyant) and instead employ "nearly neutrally buoyant" as the latter term more accurately represents the specific gravity and drifting ability of these eggs. Finally, we use diaphanous to describe the visual appearance of the egg (i.e., transparent or translucent). Eggs are still described as nonadhesive. This refined terminology follows Balon (1975, 1981) and better represents spawning behavior and physical properties of the eggs of this reproductive guild than terminology initially

applied 25 years ago (Platania and Altenbach, 1998). We provide explicit explanation of these changes, as we believe these modifications will improve consistency and accuracy of descriptions across studies concerning this unique reproductive guild.

We also extend this topic to identify species previously misassigned to this reproductive guild. Confusion regarding the reproductive behavior and egg morphology of Flathead Chub *Platygobio gracilis* occurred in the early 2000s (G. R. Wilde, pers. comm.) due to the incorrect inclusion of *Platygobio gracilis* in the following statement by Bonner and Wilde (2000): "*Hybognathus placitus*, *M. aestivalis*, *N. girardi*, **and *P. gracilis*** are members of a guild of prairie stream fishes that spawn nonadhesive, semibuoyant eggs (Platania and Altenbach, 1998)." Text in bold was not included in Platania and Altenbach (1998). Likewise, Durham and Wilde (2008) reported that *Platygobio gracilis* "broadcast semibuoyant non-adhesive eggs into the current, which drift downstream as they develop" and incorrectly attributed that information to Platania and Altenbach (1998).

Platygobio gracilis is sympatric with *Hybognathus amarus* and common in the Middle Rio Grande in New Mexico, but it was not one of the seven Rio Grande Basin leuciscids studied
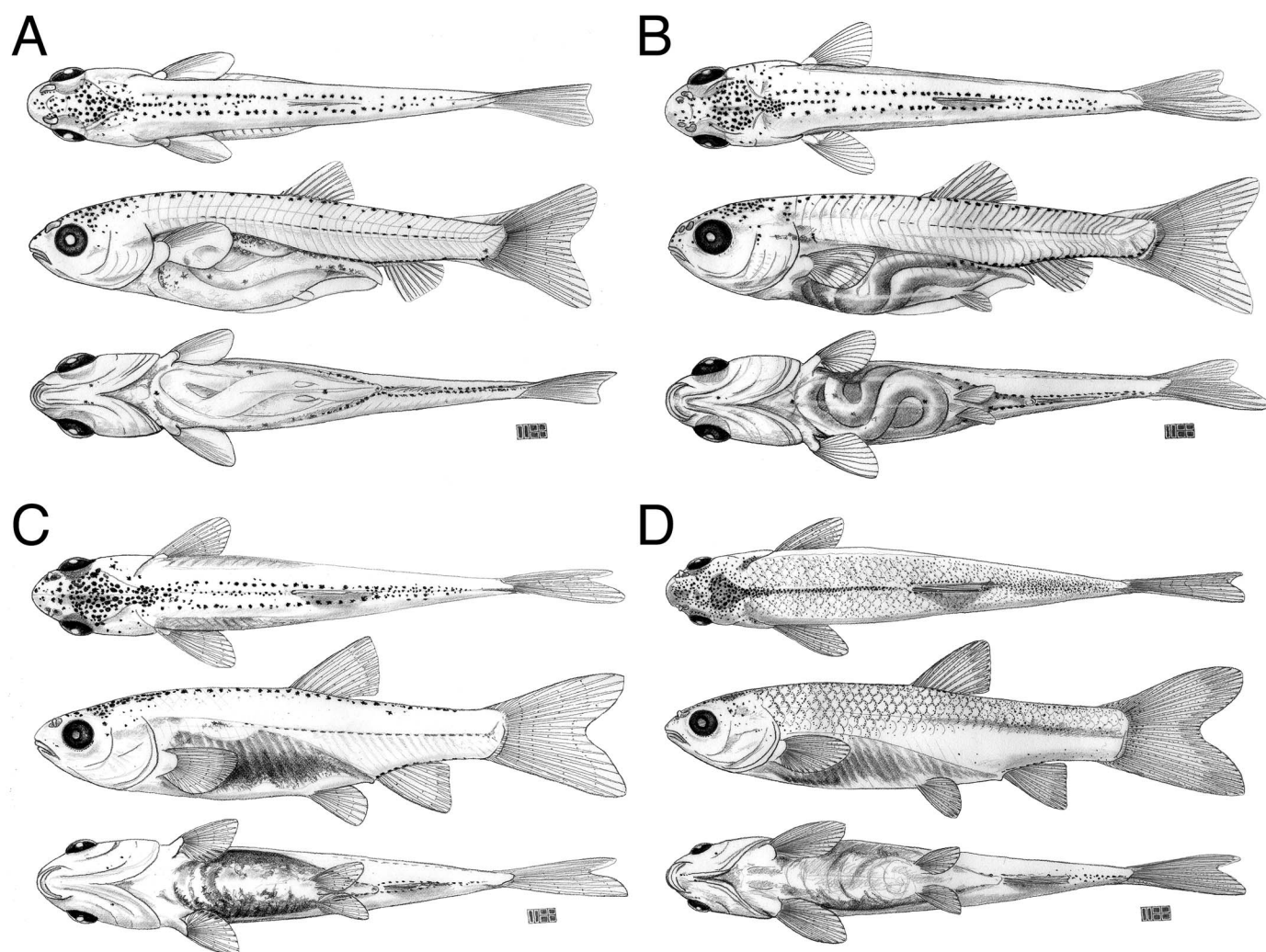
Fig. 10. Dorsal, lateral, and ventral views of *Hybognathus amarus* (MSB 49967): (A) recently transformed metalarva, 10.1 mm SL, 12.0 mm TL; (B) metalarva, 12.1 mm SL, 14.8 mm TL; (C) recently transformed juvenile, 17.6 mm SL, 21.8 mm TL; (D) early juvenile, 28.0 mm SL, 35.6 mm TL. Rectangular icon below images is the artist's stylized initials.

by Platania and Altenbach (1998) and was never reported therein as having semibuoyant eggs. Consequently, subsequent researchers disseminated the incorrect characterization of the reproduction and egg type of *Platygobio gracilis* (Rahel and Thel, 2004; Durham and Wilde, 2006, 2008; Perkin and Gido, 2011; Worthington et al., 2018). Spawning mode of *Platygobio gracilis* (e.g., pelagic, lithopelagic) remains unknown (Bestgen et al., 2016). We emphasize these differences in classification between *Platygobio gracilis* and members of this reproductive guild (e.g., *Hybognathus amarus*) because pronounced differences in egg characteristics affect reproductive success and, consequently, species-specific conservation needs (Turner et al., 2006).

Hybognathus amarus is the only extant species in the Middle Rio Grande (NM) of the reproductive guild of leuciscid pelagophils with nonadhesive, nearly neutrally buoyant, diaphanous eggs, and species-specific identification of drifting fish eggs is usually unambiguous. Over two decades of systematic reproductive monitoring of *Hybogathus amarus* in the Middle Rio Grande, we have occasionally collected live eggs of *Platygobio gracilis* concurrent with live eggs of *Hybognathus amarus*; however, several pronounced species-specific differences between egg characteristics aid in their visual identification (Fig. 11). The

perivitelline space of *Hybognathus amarus* is large and clear (i.e., diaphanous), eggs are nonadhesive, and the embryos lack any discernible pigment; these characteristics distinguish it from other resident species (Platania and Altenbach, 1998). In contrast, *Platygobio gracilis* produces small (ca. 2.5 mm diameter) nonadhesive eggs that have a high yolk-to-egg volume ratio (i.e., higher terminal velocity [settling rate] and specific gravity; Bestgen et al., 2016). Most importantly, differences in specific gravity of eggs are suspected to have profound consequences for the fate and transport of propagules (see **Implications of Egg Morphology and Embryology on Reproductive Success**).

Variations in egg morphology (specific gravity)

The specific gravity of nonadhesive, nearly neutrally buoyant diaphanous leuciscid eggs is affected by the water chemistry of the aquatic environment in which they are incubated. The semipermeable membrane of the egg allows water and ion exchange between the perivitelline space and aquatic environment (Loeffler, 1971; Ponwith and Neill, 1995), and variations in water chemistry can produce
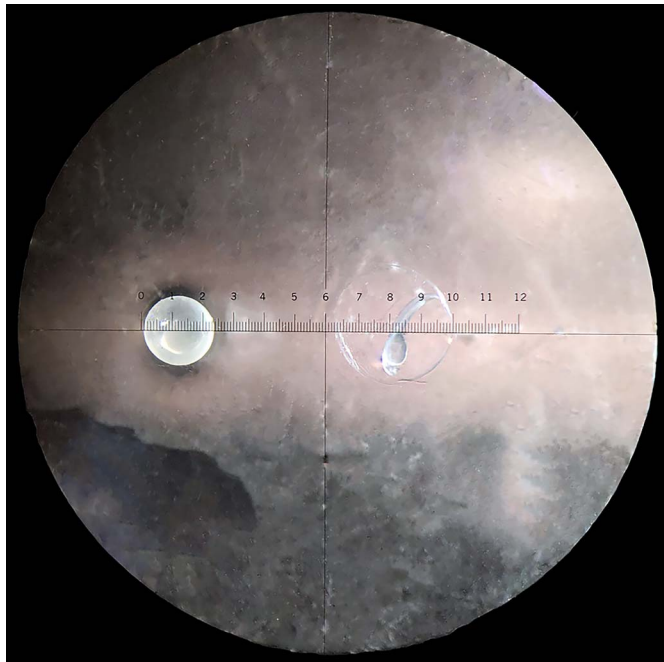
Fig. 11. Stereoscopic image of live eggs and embryos of *Platygobio gracilis* (left, 2.4 mm) and *Hybognathus amarus* (right, 3.8 mm) from the Middle Rio Grande, NM collected in May 2018. Ocular micrometer increments are 0.1 mm.

variations in egg morphology (e.g., diameter and specific gravity). To determine specific gravity of eggs of *Hybognathus amarus* we followed standardized experimental protocols used in fluid dynamics research (White and Majdalani, 2020); our tests were conducted using distilled water (20°C), the standard reference fluid for determining specific gravity (i.e., control value). This reference fluid does not replicate the physiochemical composition of water in which *Hybognathus amarus* spawns in the wild and therefore might not fully capture variation in specific gravity attributable to abiotic factors. However, use of a standardized reference fluid allows for experimental replication and provides a baseline against which other treatments can be compared.

The effects of water chemistry on the physical properties of nonadhesive, nearly neutrally buoyant leuciscid eggs have also been studied. Cowley et al. (2005, 2009) investigated the effects of salinity and sediment concentration on egg size, specific gravity, and survival of *Hybognathus amarus*. Alleman and Cowley (2006) and Alleman (2008) supplemented these studies with two pelagophils native to the Pecos River: Pecos Bluntnose Shiner *Alburnops simus pecosensis*, *Macrhybopsis aestivalis*, and two Canadian River drainage pelagophils introduced to the Pecos River: Arkansas River Shiner *Alburnops girardi* and Plains Minnow *Hybognathus placitus* (Bestgen et al., 1989). Those studies used a linear density gradient column to determine specific gravity, whereas our study determined specific gravity using an empirical relationship between terminal velocity and egg diameter.

The elevated salinity of the Pecos River, compared to the Rio Grande, is well known and regularly exceeds 3 ppt (Houston et al., 2019). Overall, the Alleman and Cowley (2006) and Alleman (2008) studies documented declining survival, reduction in egg diameter, and increased specific

gravity with increasing salinity (2–8 ppt); these effects were attributed to osmotic flux of water out of the perivitelline space (Cowley et al., 2009). For comparison, salinity in the Middle Rio Grande from April through June (i.e., spawning period of *Hybognathus amarus*) typically ranges from 0.2–0.4 ppt, with slight increases downstream likely related to lower flows and irrigations returns that tend to contain elevated salinities (0.2–0.8 ppt; Van Horn and Dahm, 2016). Given the typical range of salinity in the Middle Rio Grande, salinity is not suspected to be a limiting factor to reproduction; however, elevated salinity levels have been reported in other portions of the species' historical range, which could impair successful reintroductions of the species (Cowley et al., 2009). Additionally, egg size and specific gravity of nonadhesive, nearly neutrally buoyant eggs vary among species in this reproductive guild (Alleman and Cowley, 2006; Alleman, 2008). Variations in egg characteristics, notably specific gravity, are expected to affect the fate and transport of propagules and should be considered regarding conservation and management of these endemic species.

Effects of water temperature on hatching, growth, and survival rates

Variations in water temperature influence hatching rates and viability of eggs of *Hybognathus amarus*. Experimental water temperature treatments showed that the mortality rates of eggs and larvae were markedly higher at 15°C or 30°C, as compared with 20°C or 25°C (Platania, 2000). Therefore, it is likely that eggs spawned outside the typical spawning season (e.g., March or July), when water temperatures tend to be beyond this range, would experience increased rates of mortality. Eggs spawned in warmer water also hatch more rapidly than those spawned in cooler water (Platania, 2000), thereby reducing the drift period of the egg phase (ca. 1–3 days).

Spawning by *Hybognathus amarus*, and other members of its reproductive guild, is triggered by seasonally predictable yet variable changes in environmental conditions (Platania and Altenbach, 1998). They typically spawn shortly after rapid increases in flow during the late spring and early summer (April–June) associated with snowmelt runoff (Platania and Dudley, unpubl.). Elevated flows result in increased water velocities and depths in the main channel and inundation of channel margins and floodplains (given sufficient flow magnitude), which may function as reproductive cues. Additionally, reproductive activity could be influenced by changes in photoperiod length and water quality that accompany seasonal flow increases (e.g., increased sediment load, increased turbidity, and changes in salinity). Spawning during these periods is suspected to have facilitated successful recruitment despite erratic and often harsh abiotic conditions associated with spring floods (Osborne et al., 2005; Hoagstrom and Turner, 2013).

Like hatching rates, larval growth rates of *Hybognathus amarus* increase with increasing water temperature. Time to progress through larval developmental phases (i.e., proto-, meso-, and metalarvae) decreased with increasing water temperature (e.g., 20°C [35 days] vs. 30°C [14 days]); development was notably stunted at 15°C (Platania, 2000). Shallow habitats with minimal current (e.g., floodplains, backwaters) tend to contain elevated daytime water temperatures, which may contribute to faster growth rates. Availability of these

nursery habitats might therefore allow fish to rapidly progress through the larval developmental phase (ca. one month), leading to increased morphological development (i.e., metalarvae or juvenile), improved swimming ability, and reduced predation risk (i.e., larger body size) as flows recede and habitats become restricted to the main channel. However, elevated water temperatures (>30°C), caused by warm ambient conditions, solar radiation, and prolonged low flows during summer, likely reduce survival (Platania, 2000). In the Middle Rio Grande, water quality degradation (e.g., low dissolved oxygen concentration, high water temperature) is common during summer low flow periods (Van Horn et al., 2022). In addition to high water temperatures and potentially poor water quality, negative biotic interactions (e.g., competition, predation, and parasitism) are also presumably heightened, as the availability of suitable habitats declines and density-dependent effects increase during summer low flows.

Implications of egg morphology and embryology on reproductive success

Interactions between environmental conditions and the egg morphology and embryology of *Hybognathus amarus* likely explain its historically widespread distribution and abundance, yet these same characteristics have also made it highly susceptible to flow and habitat modifications of the Rio Grande. The species' current range, the Middle Rio Grande of central New Mexico, has been intensively modified for flood and sediment control, which has drastically reduced floodplain connectivity and complexity of instream habitats. Perhaps most importantly, the closure of Cochiti Dam in 1973 fragmented the upstream-most portion of the species' range and effectively trapped fine sediments (i.e., sand and silt) upstream, causing progressive channel degradation (i.e., incision), bed coarsening, and channel narrowing over time (Lagasse, 1980; Richard and Julien, 2003; Massong et al., 2006; Swanson et al., 2011; Mortensen et al., 2023). It appears that these changes to the aquatic environment have substantially increased the rate that propagules (i.e., eggs and larvae) are displaced downstream into unsuitable habitats (i.e., lentic conditions near and in Elephant Butte Reservoir). Our empirical work on the drift of nonadhesive, nearly neutrally buoyant eggs has demonstrated the propensity for propagules to travel considerable distances prior to hatching under contemporary flow and channel conditions (Dudley and Platania, 1999, 2007). Heightened downstream transport of eggs and larvae, along with the effects of dams and altered flows, likely contributed to the loss of *Hybognathus amarus* in the Middle Rio Grande from Cochiti Dam to Angostura Diversion Dam and to its decline from Angostura Diversion Dam to Isleta Diversion Dam (Platania and Altenbach, 1998). Systematic population monitoring efforts during October (1993–2022) indicated that the highest densities of juvenile *Hybognathus amarus* were consistently found in downstream reaches of the Middle Rio Grande (i.e., below Isleta and San Acacia Diversion Dams; Dudley et al., 2023a). One explanation for this long-term pattern of elevated densities of juveniles in downstream reaches is the cumulative longitudinal transport of propagules past instream barriers over time (Dudley and Platania, 2007).

The downstream displacement of propagules (i.e., drift) appears to be mediated by complex interactions between streamflow and channel morphology. Based on the long-term reproductive monitoring in the Middle Rio Grande (2003–2023), years with sustained high flows mid-April through mid-June (e.g., 2019 and 2023) typically had the lowest occurrence probabilities and passage rates, which suggest reduced downstream transport due to greater retention of eggs in low-velocity floodplain habitats (Dudley et al., 2023b). In contrast, years with low and fluctuating flows mid-April through mid-June (e.g., 2020–2022) were often associated with increased occurrence probabilities and passage rates (i.e., increased downstream transport). Likewise, Archdeacon et al. (2020) demonstrated that despite being reproductively capable during spring (i.e., increased Gonadosomatic Index [GSI] April–June) over a three-year study, *Hybognathus amarus* failed to recruit when spring run-off was exceptionally low (i.e., flows did not overbank). Differences in egg drift rates are likely caused by disparities in habitat complexity and availability between higher and lower seasonal flows across years (Dudley and Platania, 2007; Widmer et al., 2012). Targeted sampling of inundated floodplains during May–June has produced reproductively capable *Hybognathus amarus*, along with eggs and larvae, further supporting the importance of these ephemeral habitats for reproduction (Gonzales et al., 2014; Valdez et al., 2019, 2021). While other low-velocity nursery habitats (e.g., channel margins, backwaters, and arroyos) may result in some upstream retention of eggs and larvae during years with low or modest spring runoff (Porter and Massong, 2004a, 2004b; Pease et al., 2006), these habitats are relatively rare, particularly in incised sections of the river (e.g., below Angostura Diversion Dam; Mortensen et al., 2023). More broadly, extensive river fragmentation, flow regulation, and habitat loss in the region have led to the widespread decline or extirpation of numerous pelagic-spawning leuciscids with nonadhesive, nearly neutrally buoyant eggs (Dudley and Platania, 2007; Hoagstrom, 2015; Worthington et al., 2018).

Accordingly, the specific gravity of these eggs appears to be the most important physical characteristic influencing the downstream displacement of these propagules. For comparison, large numbers of eggs of *Platygobio gracilis* have been reported to be transported downstream in Fountain Creek, Colorado (Haworth, 2015)—this species also produces nonadhesive eggs, yet its eggs are smaller and denser (i.e., higher specific gravity than *Hybognathus amarus*) and develop more slowly than *Hybognathus amarus* (Bestgen et al., 2016). In the Middle Rio Grande of central New Mexico, *Platygobio gracilis* is common and widely distributed, with relatively stable population status across years (Turner et al., 2006; Dudley et al., 2023a), regardless of overlap in spawning periodicity with *Hybognathus amarus* and slower developmental rates. Presumably large numbers of eggs of *Platygobio gracilis* are also transported downstream in the Middle Rio Grande during spring; however, collections of drifting eggs are typically dominated by *Hybognathus amarus* (e.g., >99.5%) during years with high egg passage rates (Dudley et al., 2023b). While *Platygobio gracilis* is not a member of the same reproductive guild as *Hybognathus amarus* or *Hybognathus placitus*, we contrast these species to demonstrate the importance egg specific gravity appears to have on reproductive success and population dynamics. Nonetheless, *Platygobio gracilis* has become rare in portions of its range because of river fragmentation, flow regulation, and habitat loss (Walters et al., 2014; Bestgen et al., 2016). Considering such effects, variations in specific gravity

Fig. 12. Collection tray holding over 10,000 live eggs of *Hybognathus amarus*, which were taken in 30 min during a large spawning event in the Middle Rio Grande (NM, Socorro County, Rio Grande at Sevilleta National Wildlife Refuge, La Joya, 5 June 2018).

among species that produce nearly neutrally buoyant eggs (Alleman, 2008) might produce a range of conservation needs that are species dependent.

Beyond the egg and larval phases studied herein, *Hybognathus amarus* faces further challenges to its recovery. The duration and frequency of low flow periods in the Middle Rio Grande have increased, and substantial lengths of the river are frequently dewatered during the irrigation season (March–October; Archdeacon, 2016). Such water operations produce high mortality rates, as most fish in these segments are unable to access low flow refugia (Archdeacon and Reale, 2020). Consequently, *Hybognathus amarus* is regularly lost from substantial portions (e.g., 27–85 km from 2009–2015) of its range in the Middle Rio Grande (Archdeacon, 2016; Archdeacon and Reale, 2020; Dudley et al., 2023a). Due to the short lifespan of the species in the wild (1–2 years; Horwitz et al., 2018), marked declines in distribution and abundance can occur rapidly following consecutive years with low flows—yet the species possesses an impressive capacity to increase its distribution and abundance during years with favorable flow conditions (Dudley et al., 2023a). Since 2002, risk of extinction in the wild has been mitigated during extreme population declines through substantial augmentation with hatchery-reared fish (Archdeacon et al., 2023); however, repeated periods with elevated proportions of hatchery-origin spawners have caused negative genetic impacts to accumulate over time (Osborne et al., 2024).

River fragmentation and flow regulation across the Great Plains and American Southwest have led to the decline of numerous pelagic-spawning leuciscids, whose eggs and larvae frequently drift downstream into unsuitable habitats (Dudley and Platania, 2007; Hoagstrom, 2015; Worthington et al., 2018). However, high spring flows can help create and sustain appropriate upstream habitats (e.g., shallow, low-velocity pools and backwaters) that are essential for the successful recruitment of many freshwater fishes (Welcomme, 1979; Junk et al., 1989; Matthews, 1998), including early life phases of pelagophils (Pease et al., 2006; Turner et al., 2010; Hoagstrom and Turner, 2013; Perkin et al., 2019; Archdeacon et al., 2020; Dudley et al., 2023a, 2023b). Although many eggs of *Hybognathus amarus* (Fig. 12), and presumably larvae, are displaced downstream annually, some of these propagules are also retained upstream (Dudley and Platania, 2007; Widmer et al., 2012). Floodplain habitats likely increase the retention of these propagules and help promote the growth and survival of early developmental phases (Dudley and Platania, 1997, 2007; Magaña, 2012; Widmer et al., 2012; Medley and Shirey, 2013; Gonzales et al., 2014; Hutson et al., 2018; Tave et al., 2018; Valdez et al., 2019). These flooded nursery habitats are particularly crucial during the first month of development for *Hybognathus amarus* (ca. May–June) to help ensure its rapid and successful progression through the early larval phases (Platania, 1995, 2000).

It has been over 25 years since we first reported on the reproductive biology of several pelagophils of the Rio Grande Basin and postulated that the drift dynamics of their unique, nearly neutrally buoyant, diaphanous eggs was a key factor related to the decline and extirpation of members of this reproductive guild (Platania and Altenbach, 1998). Our subsequent work on drift dynamics of these eggs provided an empirical model that elucidated patterns of downstream transport of propagules and offered an explanation for the decline of members of this reproductive guild across the Great Plains and desert rivers of the American Southwest (Dudley and Platania, 1999, 2007). While most of our post-2000 work on this group of fishes has focused on *Hybognathus amarus*, conclusions drawn from this species are pertinent for other members of this reproductive ecotype, many of which have experienced recent and precipitous declines in their distribution and abundance (Dudley and Platania, 2007; Perkin et al., 2015; Worthington et al., 2018). Ultimately, sufficient seasonal flows, habitat complexity, and river connectivity will be required to synergistically promote the successful recruitment, survival, and long-term recovery of these unique and highly imperiled species.

DATA ACCESSIBILITY

Unless an alternative copyright or statement noting that a figure is reprinted from a previous source is noted in a figure caption, the published images and illustrations in this article

ACKNOWLEDGMENTS

LITERATURE CITED

Akaike, H. 1973. Information theory and an extension of the maximum likelihood principle, p. 267–281. *In*: Information Theory: Proceedings of the Second International Symposium. F. Csaki, B. N. Petrov, and A. Kiado (eds.). Akademiai Kiado, Budapest.

Alleman, J. C. 2008. Effects of incubation salinity on egg properties from North American cyprinids. Unpubl. M.S. thesis, New Mexico State University, Las Cruces, New Mexico.

Alleman, J. C., and D. E. Cowley. 2006. Studies on eggs of Pecos bluntnose shiner and other minnow species. Technical Report to U.S. Bureau of Reclamation, Contract No. 04-CS-40-8082.

Alò, D., and T. F. Turner. 2005. Effects of habitat fragmentation on effective population size in the endangered Rio Grande Silvery Minnow. Conservation Biology 19:1138–1148.

Archdeacon, T. P. 2016. Reduction in spring flow threatens Rio Grande Silvery Minnow: trends in abundance during river intermittency. Transactions of the American Fisheries Society 145:754–765.

Archdeacon, T. P., T. A. Diver-Franssen, N. G. Bertrand, and J. D. Grant. 2020. Drought results in recruitment failure of Rio Grande Silvery Minnow (*Hybognathus amarus*), an imperiled, pelagic broadcast-spawning minnow. Environmental Biology of Fishes 103:1033–1044.

Archdeacon, T. P., R. K. Dudley, W. J. Remshardt, W. Knight, M. Ulibarri, and E. J. Gonzales. 2023. Hatchery supplementation increases potential spawning stock of Rio Grande Silvery Minnow after population bottlenecks. Transactions of the American Fisheries Society 152:187–200.

Archdeacon, T. P., and J. K. Reale. 2020. No quarter: lack of refuge during flow intermittency results in catastrophic mortality of an imperiled minnow. Freshwater Biology 65:2108–2123.

Balon, E. K. 1975. Reproductive guilds of fishes: a proposal and definition. Journal of the Fisheries Board of Canada 32:821–864.

Balon, E. K. 1981. Additions and amendments to the classification of reproductive styles in fishes. Environmental Biology of Fishes 6:377–389.

Battle, H. I., and W. M. Sprules. 1960. A description of the semi-buoyant eggs and early developmental stages of the goldeye, *Hiodon alosoides* (Rafinesque). Journal of the Fisheries Research Board of Canada 17:245–266.

Bestgen, K. R., H. J. Crockett, M. R. Haworth, and R. M. Fitzpatrick. 2016. Production of nonadhesive eggs by flathead chub and implications for downstream transport and conservation. Journal of Fish and Wildlife Management 7:434–443.

Bestgen, K. R., and S. P. Platania. 1990. Extirpation of *Notropis simus simus* (Cope) and *Notropis orca* (Pisces: Cyprinidae) from the Rio Grande in New Mexico, with notes on their life history. Occasional Papers, the Museum of Southwestern Biology 6:1–8.

Bestgen, K. R., and S. P. Platania. 1991. Status and conservation of the Rio Grande Silvery Minnow, *Hybognathus amarus*. The Southwestern Naturalist 36:225–232.

Bestgen, K. R., S. P. Platania, J. E. Brooks, and D. L. Propst. 1989. Dispersal and life history traits of *Notropis girardi* (Cypriniformes: Cyprinidae), introduced into the Pecos River. American Midland Naturalist 122:228–235.

Bonner, T. H., and G. R. Wilde. 2000. Changes in the Canadian River fish assemblage associated with reservoir construction. Journal of Freshwater Ecology 15:189–198.

Bottrell, C. E., R. H. Ingersol, and R. W. Jones. 1964. Notes on the embryology, early development, and behavior of *Hybopsis aestivalis tetranemus* (Gilbert). Transactions of the American Microscopical Society 83:391–399.

Breder, C. M., and D. E. Rosen. 1966. Modes of Reproduction in Fishes. American Museum of Natural History, Natural History Press, Garden City, New York.

Cowley, D. E., J. C. Alleman, R. R. McShane, P. D. Shirey, and R. Sallenave. 2005. Effects of salinity and suspended sediment on physical properties of the egg of the Rio Grande silvery minnow (*Hybognathus amarus*). New Mexico Water Resources Research Institute, WRRI Technical Completion Report 334:1–19.

Cowley, D. E., J. C. Alleman, R. Sallenave, R. R. McShane, and P. D. Shirey. 2009. Effects of salinity on specific gravity and viability of eggs of a North American minnow (Cyprinidae). Scientia Marina 73:47–58.

Dudley, R. K., and S. P. Platania. 1997. Habitat use of Rio Grande Silvery Minnow. Submitted to the New Mexico Department of Game and Fish, Santa Fe, New Mexico, and to the U.S. Bureau of Reclamation, Albuquerque, New Mexico.

Dudley, R. K., and S. P. Platania. 1999. Imitating the physical properties of drifting semibuoyant fish (Cyprinidae) eggs with artificial eggs. Journal of Freshwater Ecology 14:423–430.

Dudley, R. K., and S. P. Platania. 2007. Flow regulation and fragmentation imperil pelagic-spawning riverine fishes. Ecological Applications 17:2074–2086.

Dudley, R. K., S. P. Platania, and G. C. White. 2023a. Rio Grande Silvery Minnow population monitoring during 2022. Submitted to the U.S. Bureau of Reclamation, Albuquerque, New Mexico.

Dudley, R. K., S. P. Platania, and G. C. White. 2023b. Rio Grande Silvery Minnow reproductive monitoring during 2023. Submitted to the U.S. Bureau of Reclamation, Albuquerque, New Mexico.

Durham, B. W., and G. R. Wilde. 2006. Influence of stream discharge on reproductive success of a prairie stream fish assemblage. Transactions of the American Fisheries Society 135:1644–1653.

Durham, B. W., and G. R. Wilde. 2008. Composition and abundance of drifting fish larvae in the Canadian River, Texas. Journal of Freshwater Ecology 23:273–280.

Fausch, K. D., and K. R. Bestgen. 1997. Ecology of fishes indigenous to the central and southwestern Great Plains, p. 131–166. *In*: Ecology and Conservation of Great Plains Vertebrates. F. L. Knopf and F. B. Samson (eds.). Springer New York, New York.

Fuiman, L. A. 2002. Special considerations of fish eggs and larvae, p. 1–32. *In*: Fishery Science: The Unique Contributions of Early Life Stages. L. A. Fuiman and R. G. Werner (eds.). Wiley-Blackwell, Hoboken, New Jersey.

Gido, K. B., W. K. Dodds, and M. E. Eberle. 2010. Retrospective analysis of fish community change during a half-century of land use and streamflow changes. Journal of the North American Benthological Society 29:970–987.

Girard, C. 1856. Researches upon the cyprinoid fishes inhabiting the fresh waters of the United States, west of the Mississippi Valley, from specimens in the museum of the Smithsonian Institution. Proceedings of the Academy of Natural Sciences of Philadelphia 8:165–213.

Gompertz, B. 1825. XXIV. On the nature of the function expressive of the law of human mortality, and on a new mode of determining the value of life contingencies. In a letter to Francis Baily, Esq. F. R. S. &c. Philosophical Transactions of the Royal Society of London 115:513–583.

Gonzales, E. J., D. Tave, and G. M. Haggerty. 2014. Endangered Rio Grande Silvery Minnow use constructed floodplain habitat. Ecohydrology 7:1087–1093.

Haworth, M. R. 2015. Reproduction and recruitment dynamics of flathead chub *Platygobio gracilis* relative to flow and temperature regimes in Fountain Creek, Colorado. Unpubl. M.S. thesis, Colorado State University, Fort Collins, Colorado.

Hoagstrom, C. W. 2015. Habitat loss and subdivision are additive mechanisms of fish extinction in fragmented rivers. Global Change Biology 21:4–5.

Hoagstrom, C. W., and T. F. Turner. 2013. Recruitment ecology of pelagic-broadcast spawning minnows: paradigms from the ocean advance science and conservation of an imperiled freshwater fauna. Fish and Fisheries 16:282–299.

Horwitz, R. J., D. H. Keller, P. F. Overbeck, S. P. Platania, R. K. Dudley, and E. W. Carson. 2018. Age and growth of the Rio Grande Silvery Minnow, an endangered, short-lived cyprinid of the North American southwest. Transactions of the American Fisheries Society 147:265–277.

Houston, N. A., J. V. Thomas, P. B. Ging, A. P. Teeple, D. E. Pedraza, and D. S. Wallace. 2019. Pecos River Basin salinity assessment, Santa Rosa Lake, New Mexico, to the confluence of the Pecos River and the Rio Grande, Texas, 2015. U.S. Geological Survey Scientific Investigations Report 2019–5071, Reston, Virginia.

Hutson, A. M., L. A. Toya, and D. Tave. 2018. Determining preferred spawning habitat of the endangered Rio Grande Silvery Minnow by hydrological manipulation of a conservation aquaculture facility and the implications for management. Ecohydrology 11:e1964.

Jelks, H. L., S. J. Walsh, N. M. Burkhead, S. Contreras-Balderas, E. Diaz-Pardo, D. A. Hendrickson, J. Lyons, N. E. Mandrak, F. McCormick, J. S. Nelson, S. P. Platania, B. A. Porter, C. B. Renaud, J. J. Schmitter-Soto … M. L. Warren, Jr. 2008. Conservation status of imperiled North American freshwater and diadromous fishes. Fisheries 33:372–407.

Junk, W. J., P. B. Bayley, and R. E. Sparks. 1989. The flood pulse concept in river-floodplain systems, p. 110–127. *In*: Proceedings of the International Large River Symposium (LARS). D. P. Dodge (ed.). Canadian Special Publications in Fisheries and Aquatic Sciences, Ottawa, Ontario.

Lagasse, P. F. 1980. An assessment of the response of the Rio Grande to dam construction—Cochiti to Isleta reach. Submitted to the U.S. Army Corps of Engineers, Albuquerque, New Mexico.

Loeffler, C. A. 1971. Water exchange in the pike egg. Journal of Experimental Biology 55:797–811.

Magaña, H. A. 2012. Habitat use of the Rio Grande Silvery Minnow (*Hybognathus amarus*) during a long-term flood pulse in the Middle Rio Grande, New Mexico. Environmental Biology of Fishes 95:201–212.

Mansueti, R. J., and J. D. Hardy, Jr. 1967. Development of Fishes of the Chesapeake Bay Region: An Atlas of Egg, Larval, and Juvenile Stages. Part I. University of Maryland, Natural Resources Institute, College Park, Maryland.

Massong, T. M., P. J. Tashjian, and P. W. Makar. 2006. Recent channel incision and floodplain evolution within the Middle Rio Grande, NM. Joint Eighth Federal Interagency Sedimentation Conference and Third Federal Interagency Hydrologic Modeling Conference, Reno, Nevada.

Matthews, W. J. 1998. Patterns in Freshwater Fish Ecology. Chapman and Hall, London.

Medley, C. N., and P. D. Shirey. 2013. Review and reinterpretation of Rio Grande Silvery Minnow reproductive ecology using egg biology, life history, hydrology, and geomorphology information. Ecohydrology 6:491–505.

Mollenhauer, R., S. K. Brewer, J. S. Perkin, D. Swedberg, M. Wedgeworth, and Z. D. Steffensmeier. 2021. Connectivity and flow regime direct conservation priorities for pelagophil fishes. Aquatic Conservation: Marine and Freshwater Ecosystems 31:3215–3227.

Moore, G. A. 1944. Notes on the early life history of *Notropis girardi*. Copeia 1944:209–214.

Mortensen, J. G., R. K. Dudley, S. P. Platania, G. C. White, T. F. Turner, P. Y. Julien, C. Radobenko, T. Anderson, and B. Corsi. 2023. Linking morpho-dynamics and biohabitat conditions on the Middle Rio Grande: process-linkage report III—Angostura Reach analyses. Submitted to the U.S. Bureau of Reclamation, Albuquerque, New Mexico.

Ogle, D. H., J. C. Doll, P. Wheeler, and A. Dinno. 2022. FSA: fisheries stock analysis. R package version 0.9.3. https://github.com/fishR-Core-Team/FSA

Osborne, M. J., T. P. Archdeacon, C. B. Yackulic, R. K. Dudley, G. Caeiro-Dias, and T. F. Turner. 2024. Genetic erosion in an endangered desert fish during a megadrought despite long-term supportive breeding. Conservation Biology 38:e14154.

Osborne, M. J., M. A. Benavides, and T. F. Turner. 2005. Genetic heterogeneity among pelagic egg samples and variance in reproductive success in an endangered freshwater fish, *Hybognathus amarus* (Cyprinidae). Environmental Biology of Fishes 73:463–472.

Page, L. M., K. E. Bemis, T. E. Dowling, H. E. Espinosa-Pèrez, L. T. Findley, C. R. Gilbert, K. E. Hartel, R. N. Lea, N. E. Mandrak, M. A. Neighbors, J. J. Schmitter-Soto, and H. J. Walker,Jr. 2023. Common and Scientific Names of Fishes from the United States, Canada, and Mexico. Eighth edition. American Fisheries Society, Special Publication 37, Bethesda, Maryland.

Pease, A. A., J. J. Davis, M. S. Edwards, and T. F. Turner. 2006. Habitat and resource use by larval and juvenile fishes in an arid-land river (Rio Grande, New Mexico). Freshwater Biology 51:475–486.

Perkin, J. S., and K. B. Gido. 2011. Stream fragmentation thresholds for a reproductive guild of Great Plains fishes. Fisheries 36:371–383.

Perkin, J. S., K. B. Gido, A. R. Cooper, T. F. Turner, M. J. Osborne, E. R. Johnson, and K. B. Mayes. 2015. Fragmentation and dewatering transform Great Plains stream fish communities. Ecological Monographs 85:73–92.

Perkin, J. S., T. A. Starks, C. A. Pennock, K. B. Gido, G. W. Hopper, and S. C. Hedden. 2019. Extreme drought causes fish recruitment failure in a fragmented Great Plains riverscape. Ecohydrology 12:e2120.

Platania, S. P. 1995. Reproductive biology and early life-history of Rio Grande Silvery Minnow, *Hybognathus amarus*. Submitted to the U.S. Army Corps of Engineers, Albuquerque, New Mexico.

Platania, S. P. 2000. Effects of four water temperature treatments on survival, growth, and developmental rates of Rio Grande Silvery Minnow, *Hybognathus amarus*, eggs and larvae. Submitted to the U.S. Fish and Wildlife Service, Albuquerque, New Mexico.

Platania, S. P., and C. S. Altenbach. 1998. Reproductive strategies and egg types of seven Rio Grande Basin cyprinids. Copeia 1998:559–569.

Ponwith, B. J., and W. H. Neill. 1995. The influence of incubation salinity on the buoyancy of red drum eggs and yolk sac larvae. Journal of Fish Biology 46:955–960.

Porter, M. D., and T. M. Massong. 2004a. Analyzing changes in river channel morphology using GIS for Rio Grande Silvery Minnow habitat assessment, p. 433–448. *In*: Proceedings of the Second International Symposium on GIS/Spatial Analysis in Fishery and Aquatic Sciences.

Porter, M. D., and T. M. Massong. 2004b. Contributions to delisting Rio Grande Silvery Minnow: egg habitat identification. Submitted to the U.S. Bureau of Reclamation, Albuquerque, New Mexico.

R Core Team. 2022. R: a language and environment for statistical computing. R Foundation for Statistical Computing, Vienna, Austria. https://www.R-project.org/

Rahel, F. J., and L. A. Thel. 2004. Flathead Chub (*Platygobio gracilis*): a technical conservation assessment. USDA Forest Service, Rocky Mountain Region.

Richard, G., and P. Julien. 2003. Dam impacts on and restoration of an alluvial river—Rio Grande, New Mexico. International Journal of Sediment Research 18:89–96.

Sabaj, M. H. 2020. Codes for natural history collections in ichthyology and herpetology. Copeia 108:593–669.

Schwarz, G. 1978. Estimating the dimensions of a model. The Annals of Statistics 6:461–464.

Sliger, W. A. 1967. The embryology, egg structure, micropyle and egg membranes of the plains minnow, *Hybognathus placitus* (Girard). Unpubl. M.S. thesis, Oklahoma State University, Stillwater, Oklahoma.

Snyder, D. E. 1983. Fish eggs and larvae, p. 165–197. *In*: Fisheries Techniques. L. A. Nielsen and D. L. Johnson (eds.). American Fisheries Society, Special Publication, Bethesda, Maryland.

Snyder, D. E., S. C. Seal, J. A. Charles, and C. L. Bjork. 2016. Cyprinid fish larvae and early juveniles of the Upper Colorado River Basin—morphological descriptions, comparisons, and computer interactive keys. Colorado Parks and Wildlife Technical Publication 47, Denver, Colorado.

Student. 1908. The probable error of a mean. Biometrika 6:1–25.

Swanson, B. J., G. A. Meyer, and J. E. Coonrod. 2011. Historical channel narrowing along the Rio Grande near Albuquerque, New Mexico in response to peak discharge reductions and engineering: magnitude and uncertainty of change from air photo measurements. Earth Surface Processes and Landforms 36:885–900.

Tave, D., L. A. Toya, and A. M. Hutson. 2018. Behavioral observations of the endangered Rio Grande Silvery Minnow in a conservation aquaculture facility. Croatian Journal of Fisheries 76:7–26.

Taylor, C. M., and K. B. Mayes. 2022. Impact of hydrologic alteration on Brazos River pelagophilic minnows. Transactions of the American Fisheries Society 151:474–486.

Turner, T. F., T. J. Krabbenhoft, and A. S. Burdett. 2010. Reproductive phenology and fish community structure in an arid-land river system, p. 427–446. *In*: Community Ecology of Stream Fishes: Concepts, Approaches, and

Techniques. K. B. Gido and D. A. Jackson (eds.). American Fisheries Society, Symposium Series 73, Bethesda, Maryland.

Turner, T. F., M. J. Osborne, G. R. Moyer, M. A. Benavides, and D. Alò. 2006. Life history and environmental variation interact to determine effective population to census size ratio. Proceedings of the Royal Society B: Biological Sciences 273:3065–3073.

USFWS (U.S. Fish and Wildlife Service). 1994. Endangered and threatened wildlife and plants; Final rule to list the Rio Grande silvery minnow as an endangered species. Final Rule. Federal Register 59(138):36988–36995.

Valdez, R. A., G. M. Haggerty, K. Richard, and D. Klobucar. 2019. Managed spring runoff to improve nursery floodplain habitat for endangered Rio Grande Silvery Minnow. Ecohydrology 12:e2134.

Valdez, R. A., S. A. Zipper, S. J. Kline, and G. M. Haggerty. 2021. Use of restored floodplains by fishes of the Middle Rio Grande, New Mexico, USA. Ecohydrology 14:e2262.

Van Horn, D. J., and C. N. Dahm. 2016. Rio Grande Water Chemistry Data from Bernalillo County, New Mexico (2006–2007). Sevilleta LTER Program Data. University of New Mexico Digital Repository. https://digitalrepository.unm.edu/lter_sev_data/424/

Van Horn, D. J., J. K. Reale, and T. P. Archdeacon. 2022. Water quality in three potential drought refuges in an arid-land river: assessing habitat suitability for at-risk fish species. Knowledge & Management of Aquatic Ecosystems 423:7.

von Bertalanffy, L. 1938. A quantitative theory of organic growth (inquiries on growth laws. II). Human Biology 10:181–213.

Walters, D. M., R. E. Zuellig, H. J. Crockett, J. F. Bruce, P. M. Lukacs, and R. M. Fitzpatrick. 2014. Barriers impede upstream spawning migration of Flathead Chub. Transactions of the American Fisheries Society 143:17–25.

Welcomme, R. L. 1979. The Fisheries Ecology of Floodplain Rivers. Longman, London.

White, F. M. 2006. Viscous Fluid Flow. Third edition. McGraw Hill, New York.

White, F. M., and J. Majdalani. 2020. Viscous Fluid Flow. Fourth edition. McGraw Hill, New York.

Widmer, A. M., J. J. Fluder III, J. W. Kehmeier, C. N. Medley, and R. A. Valdez. 2012. Drift and retention of pelagic spawning minnow eggs in a regulated river. River Research and Applications 28:192–203.

Worthington, T. A., A. A. Echelle, J. S. Perkin, R. Mollenhauer, N. Farless, J. J. Dyer, D. Logue, and S. K. Brewer. 2018. The emblematic minnows of the North American Great Plains: a synthesis of threats and conservation opportunities. Fish and Fisheries 19:271–307.